



**REAL-TIME HAZARDOUS CHEMICAL EMISSION RATE
MONITORING INSTRUMENT - PHASE II**

**Michael M. Carrabba, Kevin M. Spencer, Martin W. Rupich,
Michael D. Arnett, Robert W. Forney**

**EIC Laboratories, Inc.
111 Downey Street
Norwood MA 02062**

**ENVIRONICS DIRECTORATE
139 Barnes Drive, Suite 2
Tyndall AFB FL 32403-5323**

April 1996

Final Technical Report for Period April 1991 - March 1994

Approved for public release; distribution unlimited.

19961125 086

DTIC QUALITY INSPECTED 3

**AIR FORCE MATERIEL COMMAND
TYNDALL AIR FORCE BASE, FLORIDA 32403-5323**

**ARMSTRONG
LABORATORY**

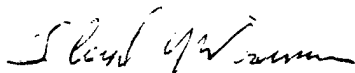
NOTICES

This report was prepared as an account of work sponsored by an agency of the United States Government. Neither the United States Government nor any agency thereof, nor any employees, nor any of their contractors, subcontractors, or their employees, make any warranty, expressed or implied, or assume any legal liability or responsibility for the accuracy, completeness, or usefulness of any privately owned rights. Reference herein to any specific commercial product, process, or service by trade name, trademark, manufacturer, or otherwise, does not necessarily constitute or imply its endorsement, recommendation, or favoring by the United States Government or any agency, contractor, or subcontractor thereof. The views and opinions of the authors expressed herein do not necessarily state or reflect those of the United States Government or any agency, contractor, or subcontractor thereof.

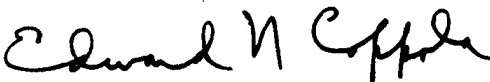
When Government drawings, specifications, or other data are used for any purpose other than in connection with a definitely Government-related procurement, the United States Government incurs no responsibility or any obligation whatsoever. The fact that the Government may have formulated or in any way supplied the said drawings, specifications, or other data is not to be regarded by implication, or otherwise in any manner construed, as licensing the holder or any other person or corporation; or as conveying any rights or permission to manufacture, use, or sell any patented invention that may in any way be related thereto.

This technical report has been reviewed by the Public Affairs Office (PA) and is releasable to the National Technical Information Service (NTIS) where it will be available to the general public, including foreign nationals.

This report has been reviewed and is approved for publication.



FLOYD L. WISEMAN, Capt, USAF
Project Manager



EDWARD N. COPPOLA, Major, USAF
Chief, Environmental Compliance
Division

REPORT DOCUMENTATION PAGE			Form Approved OMB No. 0704-0188	
<small>Public reporting burden for this collection of information is estimated to average 1 hour per response, including the time for reviewing instructions, searching existing data sources, gathering and maintaining the data needed, and completing and reviewing the collection of information. Send comments regarding this burden estimate or any other aspect of this collection of information, including suggestions for reducing this burden, to Washington Headquarters Services, Directorate for Information Operations and Reports, 1215 Jefferson Davis Highway, Suite 1204, Arlington, VA 22202-4302, and to the Office of Management and Budget, Paperwork Reduction Project (0704-0188), Washington, DC 20503</small>				
1. AGENCY USE ONLY (Leave blank)		2. REPORT DATE 20 April 1996	3. REPORT TYPE AND DATES COVERED Final Report 23Apr91 - 22Mar94	
4. TITLE AND SUBTITLE Real Time Hazardous Chemical Emission Rate Monitoring Instrument - Phase II			5. FUNDING NUMBERS F08635-91-C-0128	
6. AUTHOR(S) Michael M. Carrabba, Kevin M. Spencer, Martin W. Rupich, Michael D. Arnett and Robert W. Forney				
7. PERFORMING ORGANIZATION NAME(S) AND ADDRESS(ES) EIC Laboratories, Inc. 111 Downey Street Norwood, MA 02062			8. PERFORMING ORGANIZATION REPORT NUMBER C90020F	
9. SPONSORING/MONITORING AGENCY NAME(S) AND ADDRESS(ES) AL/EQ-OL 139 Barnes Drive, Suite 2 Tyndall AFB, FL 32403-5323			10. SPONSORING/MONITORING AGENCY REPORT NUMBER AL/EQ-TR-1994-0033	
11. SUPPLEMENTARY NOTES AL/EQS Project Manager is Capt Floyd L. Wiseman, DSN 523-6650 or (904) 283-6650				
12a. DISTRIBUTION/AVAILABILITY STATEMENT Approved for Public Release; Distribution Unlimited			12b. DISTRIBUTION CODE	
13. ABSTRACT (Maximum 200 words) <p>The purpose of this program was to develop a compact transportable monitor based on surface enhanced Raman spectroscopy (SERS) for detection of hazardous chemicals in an atmospheric environment. Our approach was to identify the adsorbates of hazardous chemicals by their vibrational spectra using SERS. The SERS spectrum is unique for each adsorbed species, can detect at the parts per million level, and can resolve gaseous mixtures. Raman spectroscopic techniques, such as SERS, are adaptable to fiber optics which serve to transfer laser light to and Raman scattering from remote sampling sites.</p> <p>Phase II continued research on hazardous gases of interest to the Air Force, particularly SO₂, monomethyl hydrazine (MMH), unsymmetrical dimethyl hydrazine (UDMH), and NO₂. In addition a complete compact prototype SERS system was fabricated and delivered to the Air Force for field deployments. The results of the Phase II program demonstrated that a practical compact SERS based monitor of hazardous gases at parts per million detection levels could be fabricated. The major advantages included real-time response, ppm detection limits and intrinsic safety. The Raman system developed can be generalized to a variety of applications, including waste analysis, groundwater analysis, biomedical testing, and online quality assurance.</p>				
14. SUBJECT TERMS Raman, Echelle, Fiber optics, Hypergolic vapors, Hazardous gases			15. NUMBER OF PAGES 54	
			16. PRICE CODE	
17. SECURITY CLASSIFICATION OF REPORT UNCLASSIFIED	18. SECURITY CLASSIFICATION OF THIS PAGE UNCLASSIFIED	19. SECURITY CLASSIFICATION OF ABSTRACT UNCLASSIFIED	20. LIMITATION OF ABSTRACT UNLIMITED	

PREFACE

This report was prepared by EIC Laboratories, Inc., 111 Downey Street, Norwood, MA 02062, under Contract No. F08635-91-C-0128, for the Headquarters Air Force Engineering and Services Center, Directorate of Engineering and Services Laboratory (HQ AL/EQS-OL), Tyndall Air Force Base, Florida 32403-6001.

This final report describes the detection of hazardous gaseous vapors by surface-enhanced Raman spectroscopy (SERS) in atmospheric environments; determination of the appropriate SERS substrate fabrication methods; fabrication of a monitoring instrument for field use; laboratory testing of the field prototype; and assesses the capabilities and limits of the delivered prototype.

This work was performed between April 1991 and March 1994. The initial AL/EQS-OL Project Officer was Captain Michael T. Moss. The final AL/EQS-OL Project Officer was Captain Floyd L. Wiseman.

EXECUTIVE SUMMARY

A. OBJECTIVE

The purpose of this program was to develop a compact transportable monitor based on surface-enhanced Raman spectroscopy (SERS) for detection of hazardous chemicals in an atmospheric environment.

B. BACKGROUND

Our approach was to identify the adsorbates of hazardous chemicals and hypergolic propellants by their vibrational spectra using SERS. The SERS signal corresponds to the vibrational spectrum of a molecule adsorbed on a metal surface. The SERS spectrum is obtained from the Raman scattering off the substrate using a visible or near infrared (NIR) laser source and is unique for each adsorbed species. The SERS technique is capable of detection at the parts per billion level and can simultaneously resolve gaseous mixtures. Raman spectroscopic techniques, such as SERS, are adaptable to fiber-optic utilization. The fiber-optics can serve to transfer laser light to and Raman scattering from a remote sampling site.

C. SCOPE

The Phase II program continued the initial research on hazardous gases of interest to the Air Force. The gases emphasized were the hazardous gas sulfur dioxide (SO_2) and the hypergolic propellants monomethyl hydrazine (MMH), unsymmetrical dimethylhydrazine (UDMH), and nitrogen dioxide (NO_2), a decomposition product of the nitrogen tetroxide oxidizer. The Phase II program also concentrated on the fabrication and delivery of a complete compact prototype SERS system which can be utilized by Air Force personnel in nonlaboratory environments.

D. METHODOLOGY

SERS substrates were fabricated electrochemically and by vacuum deposition. A portion of the fabricated substrates were also oxidized. Multiple substrate fabrication processes were studied to determine the most appropriate substrate in terms of sensitivity and reproducibility. In addition, silver, gold, copper, and iridium metals were employed as the SERS substrates. The laser wavelengths were also varied to determine which would be most sensitive to SERS enhancement.

Diode lasers were chosen as the laser source for the portable instrument. Several diode lasers from various manufacturers were tested. An echelle spectrograph was fabricated and coupled to a two-dimensional charge coupled device (CCD) to collect the entire Raman spectral range at high resolution. To allow remote detection, a fiber-optic Raman probe was fabricated which employs filtering techniques for maximization of the spectral signal-to-noise ratio.

E. TEST DESCRIPTION

All SERS substrates were tested in a specially prepared cell. The SERS substrate fit into the back side of the chamber and the SERS active side faced a quartz window through which the

laser light could reach the substrate surface. Teflon® gas lines connected to the cell permitted hazardous gases to flow across the SERS substrate. The scattered SERS signal was collected through the quartz window.

Diode lasers were tested for stability and background radiation through the collection of the diode laser line on the CCD camera. Variations in wavelength and power as a function of temperature and input current were conducted. Throughput tests were performed on the Raman probe and standard Raman spectra were collected. Spectra were collected from the assembled prototype and compared to spectra obtained on other laboratory instruments.

F. RESULTS

Vacuum and electrochemically prepared substrates were determined to be applicable for detection of hazardous gases in the high ppb-low ppm range. Neither technique appeared to be more advantageous for substrate reproducibility. Fast response times, substrate reversibility and renewability were demonstrated. Roughening and oxidation conditions of the SERS substrates could be varied to optimize detection of a specific hazardous gas.

Diode lasers were determined to be unstable due to optical feedback and had to be optically isolated. A 100-mW 775-nm device was chosen for utilization in the prototype instrument. Testing of the prototype unit demonstrated that remote detection of the hazardous gases of interest was feasible.

G. CONCLUSIONS

The results of the Phase II program demonstrated that a practical compact SERS-based monitor of hazardous gases could be fabricated. The major advantages include real-time response, simultaneous multicomponent detection, low detection limits and intrinsic safety. The Raman system developed can be generalized to a variety of applications, including waste analysis, groundwater analysis, biomedical testing, and online quality assurance.

H. RECOMMENDATIONS

The SERS-based instrument can be utilized for field detection of gases. Improvements in detection of hazardous gases in the atmosphere should proceed along three paths. The first path emphasizes the need to expand the SERS database of hazardous gases. The second path would concentrate on manufacturing methods for optimization of SERS substrate repeatability and sensitivity. The third path would investigate instrumental improvements to increase the monitor sensitivity.

TABLE OF CONTENTS

Section	Page
I INTRODUCTION	1
A. INTRODUCTION	1
B. BACKGROUND	1
C. SCOPE	4
II SERS ANALYSIS OF HAZARDOUS VAPORS	6
A. EXPERIMENTAL	6
B. SERS SPECTRA OF THE HAZARDOUS GASES OF INTEREST	9
C. INVESTIGATION OF AN INTERNAL STANDARD	9
D. INVESTIGATION OF A PHTHALOCYANINE OVERCOATING	12
E. VACUUM DEPOSITION VERSUS ELECTROCHEMICAL SUBSTRATES	16
F. SERS REPRODUCIBILITY TESTING	18
G. SERS WAVELENGTH AND SUBSTRATE TESTING	20
III FABRICATION OF A PROTOTYPE SERS INSTRUMENT	23
A. DIODE LASER EVALUATION	23
B. FABRICATION AND EVALUATION OF THE PROTOTYPE ECHELLE SPECTROGRAPH	24
C. FABRICATION AND EVALUATION OF SERS INSERT	28
D. FABRICATION AND EVALUATION OF FIBER-OPTIC RAMAN PROBE	29
IV EVALUATION OF THE PROTOTYPE INSTRUMENT	32
V CONCLUSIONS	40
VI RECOMMENDATIONS	41

LIST OF FIGURES

Figure		Page
1	Comparison of Unfiltered Probe and EIC Filtered Raman Probe	5
2	Schematic of the Gas Flow Cell	6
3	Schematic of the Vapor Generator, Gas Delivery and Analysis System.....	7
4	SERS Spectra of the Hazardous Gases of Interest.....	10
5	Raman Spectra of Diamond-Impregnated Silver, Copper, and Gold SERS Substrates	11
6	SERS Spectrum of NO ₂ on a Diamond-Impregnated Silver SERS Substrate	12
7	SERS Spectra of Cobalt and Lead Phthalocyanine in Air	13
8	SERS Spectrum of Phthalocyanine as a Function of Coating Thickness	14
9	SERS Spectrum of Phthalocyanine as a Function of Wavelength.....	15
10	SERS Spectrum of NO ₂ on a Copper Phthalocyanine Silver Substrate.....	16
11	SERS Spectrum of 48 ppm NO ₂ on a Plasma-Oxidized Silver Substrate	18
12	SERS Spectrum of UDMH Obtained on Silver Substrates using Galvanic and Potentiostatic Oxidation.....	19
13	Long Term Evaluation of MMH Signal Intensity	20
14	The SERS Spectrum of SO ₂ as a Function of Wavelength.....	21
15	The SERS Spectrum of NO ₂ as a Function of Wavelength	22
16	Schematic of the Prototype Echelle	26
17	Spot Size of the Echelle Spectrograph.....	26
18	Image of the White Light Spectrum	27
19	Schematic of the SERS Insert.....	28
20	Fiber-Optic SERS Spectrum of 48 ppm SO ₂ with a 514.5 nm Source	29

LIST OF FIGURES

Figure		Page
21	Fiber-Optic SERS Spectrum of 5 ppm SO ₂ with a 514.5 nm Source	30
22	Schematic of the Fiber-Optic Raman Probe	30
23	SERS Spectrum of 14 ppm UDMH.....	31
24	Normalized White Light Spectrum Collected with the Prototype System...	33
25	Emission Spectrum of Neon Collected with the Prototype System	34
26	Emission Spectrum of Mercury Collected with the Prototype System	34
27	Emission Spectrum of Krypton Collected with the Prototype System.....	35
28	Emission Spectrum of Xenon Collected with the Prototype System	35
29	Emission Spectrum of Argon Collected with the Prototype System.....	36
30	Raman Spectrum of Naphthalene Collected with the Prototype System.....	36
31	Raman Spectrum of CCl ₄ Collected with the Prototype System	37
32	SERS Spectrum of 150 ppm UDMH Collected with the Prototype System	38
33	SERS Spectrum of 48 ppm NO ₂ Collected with the Prototype System	38
34	SERS Spectrum of 48 ppm SO ₂ Collected with the Prototype System	39

(The Reverse of This Page Is Blank)

SECTION I

INTRODUCTION

A. INTRODUCTION

The objective of the Phase II program was to develop compact transportable instruments for detection, identification, and quantification of hazardous chemicals in the atmosphere. Emissions of hazardous gases associated with flight operations, such as sulfur dioxide, nitrogen tetroxide, and unsymmetrical dimethylhydrazine (UDMH), can present significant threats to the safety of civilian and Air Force personnel. The toxic nature of these hazardous materials requires techniques for remote monitoring of the environment. Monitoring must be for appearance of contaminants, probing potential emission sources, and accurately assessing the source and downwind concentrations after an accidental release of hazardous chemicals.

Our approach was to identify adsorbates of these hazardous airborne chemicals by their unique vibrational spectra, using surface-enhanced Raman spectroscopy (SERS). SERS can be 10^6 to 10^8 more sensitive than normal Raman spectroscopy, and thus has the potential for detection in the parts per billion range. The SERS spectrum is obtained from the Raman scattering of the molecule adsorbed onto certain "SERS active" substrates.

We also chose to utilize fiber-optics and diode lasers to enable Raman spectroscopy to become a field-deployable technique. The SERS substrate may be placed in a remote location and interrogated via fiber-optics which transmit laser light to the substrate and return to the Raman system with the SERS signal. Diode lasers require no special utility requirements and are very compact. Coupled with a compact spectrograph, the diode laser and fiber-optic SERS probe enable rapid field deployment. The Raman system could be placed in a military vehicle and driven to sites where the SERS probes are permanently deployed for environmental sampling.

B. BACKGROUND

The Raman experiment consists of exciting a sample with monochromatic laser light, returning the scattered light to a spectrograph and obtaining the spectrum with an appropriate light detection device at the spectrograph's focal plane. Typically, in unenhanced Raman spectroscopy, about $10^{-3}\%$ of the intensity of laser light impinging on a molecule will be scattered, mostly elastically at the excitation frequency. However, about 1% of the scattered light will be at frequencies corresponding to combinations of the exciting light and the molecular vibrational frequencies (the Raman effect). Thus, spectral resolution of the scattered light will yield a "fingerprint" of the molecule consisting of sharp lines which, like the infrared spectrum, give information about the chemical bonding and structure. Furthermore, the sharpness of the lines makes possible simultaneous identification of several species. The main disadvantage of unenhanced Raman spectroscopy is its insensitivity. It becomes experimentally very difficult to measure spectra at concentrations below 1 percent. An enhanced Raman technique, such as SERS, is essential to approach the detection limits necessary for contamination analysis.

The SERS phenomenon was first reported by Fleischmann and co-workers (Fleischmann, 1974) who described a very large enhancement of the Raman signal from pyridine when adsorbed onto an electrochemically roughened silver surface. Quantitative studies of Raman scattering from molecules adsorbed onto electrochemically roughened substrates of highly reflective metals or in solutions of their metal colloids indicate that the SERS enhancement factor can be as high as 10^6 - 10^8 compared to the signals of adsorbates on nonactive or smooth surfaces. Although SERS has been observed on many metallic substrates, the most active appear to be gold, silver, and copper. The various types of SERS active substrates include colloids, electrodes, coated microspheres, island films, and lithographically prepared posts, with the most prevalent being electrodes and colloids.

The two mechanisms developed to explain the SERS phenomenon have been categorized as the charge transfer and electromagnetic effects. The actual enhancement is generally attributed to a combination of the two theories. Several reviews have been written describing the theories of SERS (Chang, 1982; Pockrand, 1984). There is also a more recent review of the SERS technique and its experimental aspects (Garrell, 1989).

The selectivity of the SERS technique depends on several factors. The first is the wavelength of excitation. Each metal substrate has an optimum enhancement based on the energy (wavelength) of the incident photons. The second factor is the ability of the molecule to adsorb onto the metal surface. To observe SERS enhancement, the molecule must be confined approximately to a distance of < 20 nm from the metal surface. Studies have shown that the free energy of adsorption, ΔG_{ads} , depends both on the structure of the gaseous adsorbate and the substrate. This dependence results in a chemical selectivity in the adsorption process (Gileadi, 1977). If a SERS active substrate is exposed to an environment containing a mixture of compounds, only those that preferentially adsorb onto the substrate surface will be detected. Catalytic and electrochemical research has shown that hydrocarbons containing π orbitals or electron donors, such as nitrogen, oxygen, or sulfur, are readily adsorbed onto metal surfaces from aqueous solutions (Bond, 1962).

We have found that roughened metal substrates generally display little affinity for the adsorption of the majority of gaseous molecules on SERS active sites. However, the sensitivity could be greatly improved by the creation of a metal oxide overlayer on the roughened SERS substrate. Gold and silver have been found to exhibit high SERS activity for a variety of adsorbed gases (Carrabba, 1988; Carrabba, 1988). Of particular significance, the adsorption of numerous gases on the metal oxide surfaces is a reversible process under ambient conditions. Two key properties of the metal oxides which are believed to control the adsorption of gaseous molecules on the metal oxides are their oxidation/reduction characteristics as well as acid/base properties of the substrate.

A surface metal interaction can lead to more than a simple adsorption. Metals have been utilized as catalysts for a variety of reactions, introducing the possibility of formation of new chemical species. In general, the SERS spectrum looks similar to the standard Raman spectrum with only minor shifts in spectral frequencies. If an unexpected spectrum is obtained, a reaction has occurred at the surface and the SERS spectrum of an adsorbed product has been collected. One striking example is the polymerization of trichloroethylene on a copper electrode (Carrabba, 1992).

The enhanced selectivity and sensitivity of SERS can only be utilized for detection of hazardous gaseous emissions if it can be easily deployed. Despite the many analytical advantages which NIR Raman spectroscopy offers, the technique has often been ignored, mainly due to the cost and complexity of the equipment necessary for a Raman system. However, recent advances at EIC in both compact spectrographs (Carrabba, 1990) and fiber-optic sampling (Carrabba, 1992) have exposed Raman spectroscopy to field applications. Manufacturer advancements have created a variety of useful laser systems which can be utilized in the field without specialized utility requirements.

Since Raman measurements are collected in terms of frequency differences from the laser source, measurements can theoretically be made regardless of the initial wavelength of the excitation light. Raman spectra have been obtained using excitation sources ranging from 200-nm to 1.3- μ m. The choice of laser source is then dependent on availability of portable source and the sensitivity of the gaseous substrate at a particular energy. The most appropriate laser sources are the air-cooled argon, the frequency-doubled Nd:YAG, and the solid-state diode laser. The former two choices emit light at laser wavelengths (514.5-nm, 532-nm) where a SERS enhancement is not observed for the gaseous species of interest. SERS sensitivity was shown in the 650-nm range during the Phase I program, indicating that utilization of diode lasers in the 670-700-nm range was feasible. Diode lasers in the 770-800-nm range have higher power levels and were also worthy of investigation.

There are numerous compact spectrographs which may be utilized for field applications. However, none meet the criteria which we desired for the current application. First, other spectrographs available at the start of this program had moving parts which could lead to system misalignment. Second, the ideal spectrograph should allow collection of a wide range at high resolution simultaneously, so there is no need to have to modify the spectrograph by changing gratings. A rugged spectrograph which provides all the desired information allows nonspecialists to utilize the Raman system without rigorous training, making the technique more accessible to the general public.

Our system employs an echelle grating rather than the traditional dispersive grating. In effect, the echelle spectrograph is able to concentrate most of the available light into multiple coincident spectral orders with high dispersion. The multiple spatially overlapping orders are then separated by a cross-dispersing element (a pair of prisms in the current design) and are projected as stacked segments onto the focal plane. Recent advances in CCD detector technology now permit the simultaneous detection of these multiple orders, theoretically permitting the acquisition of a complete (50-4000-cm⁻¹) Raman spectrum in a single measurement with high resolution. The echelle spectrograph can be designed to have minimal optical aberrations such that the resolution of the system is limited only by the entrance slit and the CCD pixel element density. For remote sensing applications, the fiber itself may serve as the entrance slit.

A critical component for field deployment is a system which can transfer information from the remote location to the central system. For this technique where light is the information medium, a fiber-optic probe is desired. Two types of Raman probes can be categorized as filter and nonfilter; both of these have undergone extensive testing at EIC (Carrabba, 1988; Carrabba, 1989; Carrabba, 1989; Carrabba, 1991). The unfiltered type consists of a single optical fiber transporting the laser light to the sample surrounded by one or more fibers which would transport the resultant Raman

signal back to the spectrometer. Since the bare fiber emits light in a conical fashion, the light is not focused and Raman collection depends on the overlapping of the cones of the fibers. The end result is an inefficient system which can be partially compensated for through the addition of extra collection fibers with the limit being the number of optical fibers that can be imaged onto the spectrograph slit.

A major problem with probes which contained bare silica fibers is that the fibers themselves give rise to Raman scattering which interfere with the spectrum (Angel, 1990; Carrabba, 1992). The result is that any silica Raman bands produced in the excitation fiber can also be reflected into the collection fibers. In addition, since only bare fibers are employed, there is no method to filter out the elastically scattered laser line signal (10^6 times more intense than Raman signals) until the light reaches the spectrometer. Therefore, the scattered laser light can interact with the silica fiber used for collection and produce Raman bands from the silica itself.

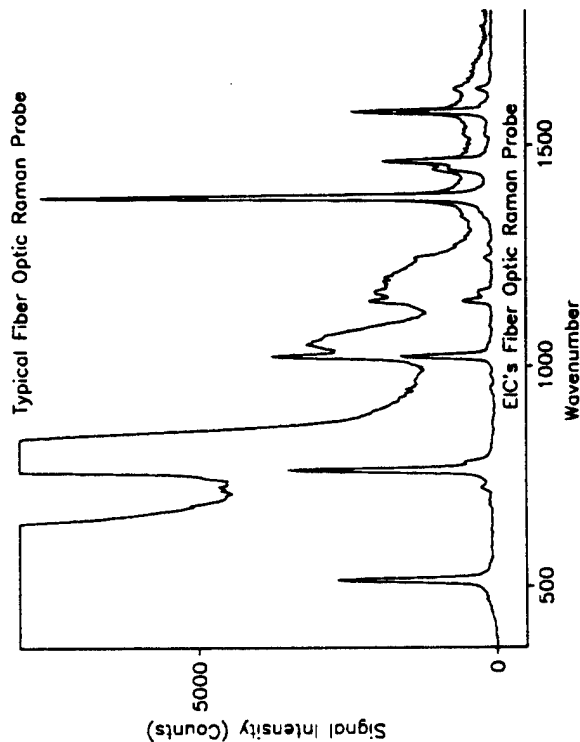
Bare fiber arrangement may be acceptable for small lengths (< 1 meter) of fibers where the silica Raman signals are weak and low detection limits are not required. However, for fiber-optic lengths of >5 m or low detection limit Raman analysis the silica noise will become so severe that detection of the desired Raman signals becomes difficult. The disadvantages of an unfiltered Raman probe when compared to a filtered Raman probe are displayed in Figure 1A.

The EIC filtered probe design (Figure 1B) utilizes the same lens for delivery of the excitation source to the sample and collection of the Raman signal. This is also called 180° backscattering. The Raman signal is separated from the scattered laser light within the Raman probe through the efficient use of a dichroic filter followed by a dielectric edge filter. This probe is easier to align and has a higher signal throughput since there is total overlap between the excitation and collection cones. This 180° backscattering design was employed exclusively during the Phase II program.

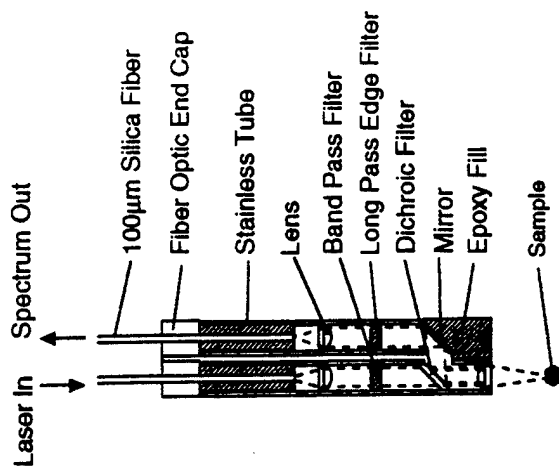
C. SCOPE

The major technical issues addressed during the Phase II program were:

- To investigate the utilization of an internal standard for normalization of the SERS signal.
- To determine the optimum manufacturing process for SERS substrate reproducibility and sensitivity.
- To determine SERS sensitivity for the studied hazardous gases at NIR wavelengths.
- To determine the most appropriate metallic substrate at NIR wavelengths.
- To determine the most appropriate diode laser source for the prototype instrument.
- To develop and evaluate the NIR echelle spectrograph.
- To fabricate a fiber-optic Raman probe at the diode laser wavelength.
- To fabricate an insert to restrict the SERS substrate at the focal volume of the Raman probe.
- To evaluate the performance of the fiber-optic SERS assembly.
- To evaluate and finalize the deliverable prototype.



EIC Fiber Optic Raman Probe U.S. Patent 5,112,127



EIC Laboratories, Inc.

A

B

Figure 1.

A - Comparison of an Unfiltered (Top) Raman Probe and an EIC Filtered 180° Backscattering Raman Probe. Note the Large Background in the Unfiltered Probe due to Silica Raman Bands Present in the Fiber. B - Schematic Diagram of the EIC 180° Backscattering Fiber-Optic Raman Probe.

SECTION II

SERS ANALYSIS OF HAZARDOUS VAPORS

A. EXPERIMENTAL

1. SERS Instrumentation

All experiments were performed at the EIC Laboratories' laser spectroscopy facility. Initially, SERS spectra were collected on commercial Raman spectrographs (Spex Triplemate, ISA HR320) using incident laser radiation from argon, krypton, dye, and diode lasers (Coherent, Spectra Diode Laboratories). Liquid-nitrogen-cooled CCDs were utilized for detection of signals. The CCD (Photometrics, Ltd.) utilized for the majority of the experiments incorporates a 1-inch long CCD chip (EEV 88131) to allow for an adequate spectral range to be collected simultaneously. A CCD (Photometrics, Ltd.) with a 1/2-inch long chip was employed for some of the wavelength dependence studies. Raman spectral collection was performed using standard software routines written into the Photometrics software. The spectra were stored, manipulated and plotted using Lab Calc[®] software.

A surface-enhanced Raman spectroscopy (SERS) gas-phase excitation cell was fabricated for use in the Phase I program. A schematic of the cell is shown in Figure 2. The cell body was constructed entirely of Teflon[®] to minimize adsorption or reaction of the chemical vapors. The optical window consisted of a 2.54-cm diameter quartz plate installed in the bottom of the cell body. The cell is completely sealed with respect to the outside environment. The cell permits the rapid and reproducible positioning of the substrates.

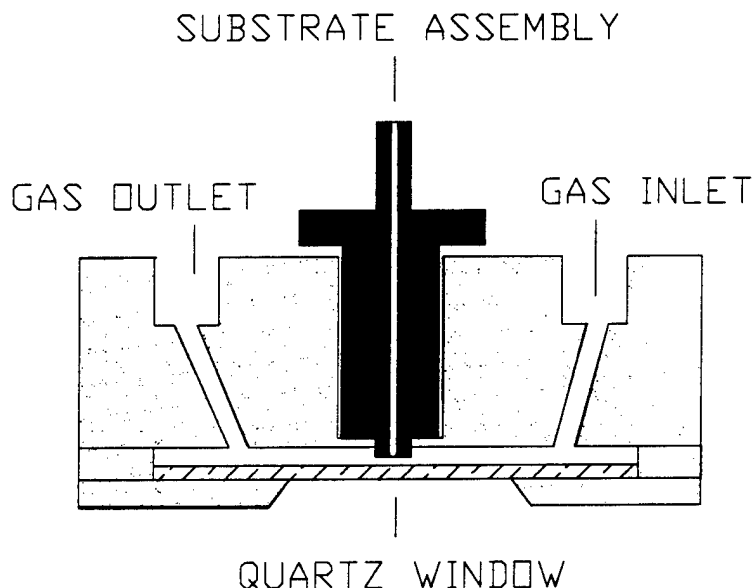


Figure 2. Schematic of the SERS Excitation Cell Fabricated for the Phase I Measurements.

2. Gases

The principal hazardous gases employed for the Phase II program were NO_2 , SO_2 , monomethyl hydrazine (MMH), and unsymmetrical dimethylhydrazine (UDMH). NO_2 and SO_2 were purchased from Scott Specialty Gases as 48-ppm in N_2 . Subsequent dilutions were accomplished with a Matheson gas mixer. The gases were diluted with O_2 , a necessary component for SO_4^{2-} detection. With the gas mixer, 20:1 dilutions could be accurately achieved.

Monomethyl hydrazine and UDMH were obtained as liquids from Aldrich and were transferred to a Kin-Tek® 570 C Gas Standards Generator. The Kin-Tek® is a gas permeation system in which the MMH and UDMH concentrations were verified by impinger collection of the vapor stream in 0.1 N H_2SO_4 and coulometric analysis. A schematic of the MMH generator, the SERS cell, the laser, and the CCD detector is illustrated in Figure 3. All sampling lines from any of the gas tanks to the SERS cell consisted of 4-mm outside diameter Teflon® tubing.

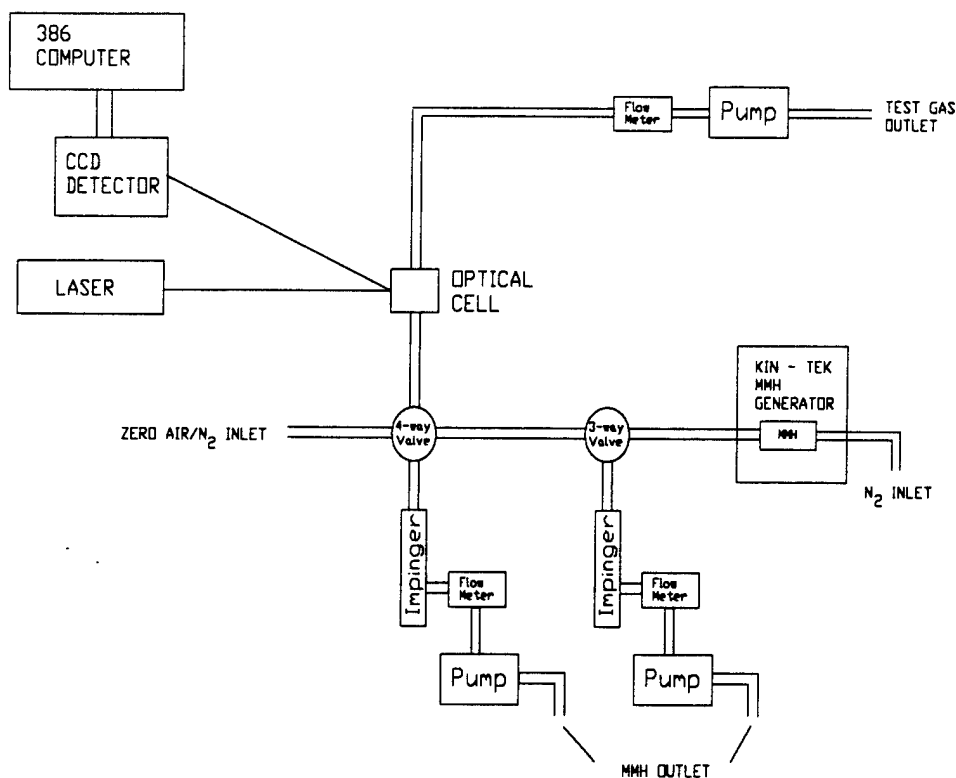


Figure 3. Schematic of the Vapor Generator, Gas Delivery and Analysis System.

3. Electrodes

Electrodes utilized for the electrochemical process were prepared by sealing a 1-mm wire of the base metal into a glass capillary. The electrodes that were utilized for the Phase II experiments were CuO , $\text{Cu}_2\text{O}/\text{Cu}$, Cu , Ag_2O , AgO/Ag , Ag , AuO/Au , and Au . The preparation of the metal oxide substrates from the base metal assemblies was carried out by electrochemical

techniques. The metal substrate surfaces were initially roughened by potentiostatic cycling in either aqueous KCl or aqueous AgNO_3 . The potential limits, the number of cycles, and the salt concentrations were adjusted as appropriate for each metal. In addition, the cycling parameters for a particular metal could be varied slightly to increase sensitivity to a particular hazardous gas. The potentiostatic cycling results in the formation of a highly roughened metal surface that has the morphology required for SERS activity.

The roughened silver surface was converted to the oxide by potentiostatic oxidation in 1.0 M KOH. The current potential curve obtained by oxidation of a silver electrode in 1.0 M KOH indicates the formation of two types of silver oxide. The first peak corresponds to the formation of Ag_2O while the second corresponds to the formation of AgO . By controlling the potential of the substrate, it is possible to control the composition of the metal oxide. Similar procedures were used for the fabrication of other oxide substrates. Electrochemical procedures were carried out with a Princeton Applied Research Model 273 potentiostat interfaced to a laboratory computer or a Pine Instrument RD 4 potentiostat.

4. Vacuum Deposition

Electrochemically prepared oxide substrates lose activity over a period of time. The activity of the electrode can range from minutes to weeks and is highly dependent upon experimental conditions. Preliminary results suggest that the photo-induced decomposition from the laser excitation source is a primary factor. One method of improving the stability of the silver oxide (or other substrates) substrate is to deposit the silver oxide on a nonsilver substrate whose morphology is not affected by thermal cycling and which does not react with the silver oxides. The use of inert substrates is expected to eliminate or reduce changes in the surface morphology while the absence of a $\text{Ag}_2\text{O}/\text{Ag}$ interface will decrease or eliminate the photo-induced decomposition of Ag_2O . In addition to more stable surfaces, vacuum deposition methods (sputtering and thermal evaporation) are ideally suited for the preparation of highly controlled surface morphologies. The control of the morphology will help in producing SERS substrates which are reproducible and can maintain calibration.

The technique involved the deposition of the oxides onto a previously roughened substrate of Ag and Au. Since the enhancement comes from the base metals of Ag and Au, the vacuum deposition method has extended our investigation into other oxide substrates which were previously uncharacterized. Various thin-film vacuum-deposition equipment were used to produce different oxide coatings. Our thin-film fabrication systems include capabilities for RF (radio-frequency) and DC sputtering, ion-beam processing, and thermal evaporation. The thermal evaporation systems are equipped with thickness/rate monitors for accurate determination of the thickness of the oxide coating. For the sputtering method, the thickness was determined by measuring the amount deposited onto a glass slide during the sputtering. The thickness was determined with a Sloan Dektak[®] surface profile measuring system. Two sample coatings and the method for producing the coatings are listed below. Some variations on the pressures and thickness from these standard examples were performed.

Ag₂O - Method (I)

Sputtering Using a Ag Target:

Base pressure	1.4×10^{-4} torr
Sputtering pressure	1.4×10^{-2} torr
Sputtering gas	O ₂
Sputtering power	4 watts
Sputtering rate	230 Å/min
Sputtering duration	1 min
Thickness	23 nm

Ag₂O - Method (II)

Sputtering Using a Ag Target:

Base pressure	1.2×10^{-4} torr
Sputtering pressure	4×10^{-2} torr
Sputtering gas	O ₂
Sputtering power	8 watts
Sputtering rate	N/A
Sputtering duration	5 min
Thickness	23 nm

B. SERS SPECTRA OF THE HAZARDOUS GASES OF INTEREST

The SERS spectra of the four hazardous gases (UDMH, MMH, NO₂, and SO₂) were collected during the Phase I program. As a point of reference, the SERS spectrum for each of these gases is displayed in Figure 4.

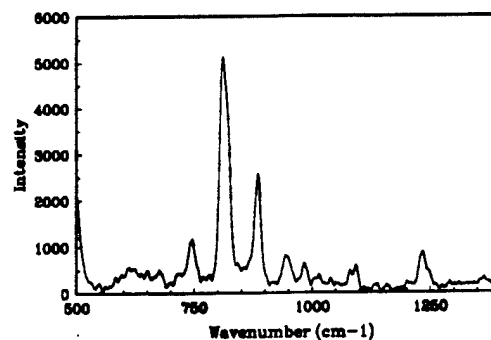
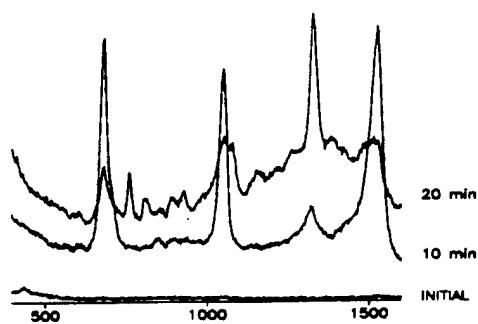
C. INVESTIGATION OF AN INTERNAL STANDARD

One method by which the SERS technique can be made to be more quantitative is to encapsulate onto the substrate surface a compound which would always maintain a constant Raman signal. The SERS intensities could be ratioed against the signal strength of this Raman standard to remove questions regarding alignment variations. In addition, constant observation of a Raman signal would assure the end user of the functionality of the system in situations where hazardous gas concentrations are below detection limits. The standard should have sufficient Raman signal to determine the system functionality while not masking the Raman band(s) of interest.

During the Phase II program, we tested the feasibility of fabricating SERS substrates with incorporated internal standards. The material we investigated as an internal standard was diamond, whose characteristic Raman feature is a sharp peak at 1332 cm⁻¹. Diamond has a unique Raman spectrum which should not interfere with the hazardous gases. Diamond appeared to be an excellent choice for an internal standard, since it is chemically inert and has only a single Raman band in the region of interest. In powdered form, diamond is economical (~\$50/g) and may be used in dilute quantities.

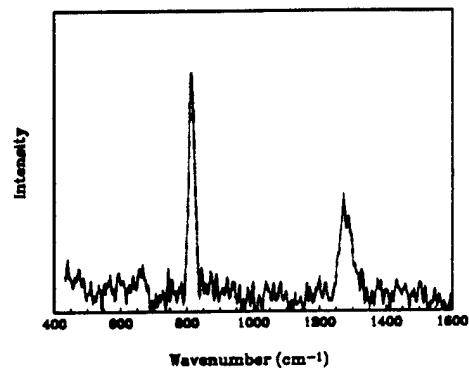
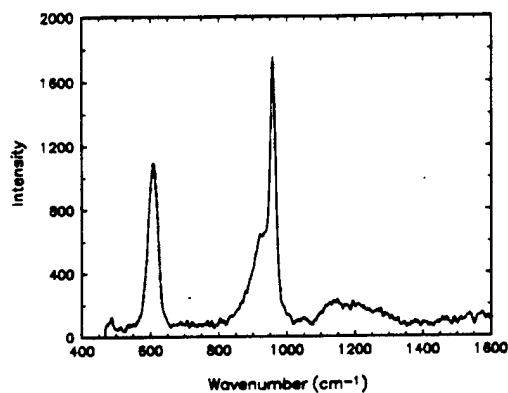
Finely dispersed diamond particles were imbedded into silver, gold, and copper substrates prior to roughening. The substrates were then electrochemically roughened and oxidized to form the SERS substrates for the hazardous gases. At each point in the process, the Raman spectrum of the surface was obtained. The resulting spectra for all three substrates are displayed in Figure 5. The imbedded diamond showed that it was capable of surviving the electrochemical roughening and oxidation cycles. The changes in diamond signal strength are a problem of electrode alignment and not an intrinsic change in diamond signal strength.

UDMH on AgOX (800013,14,15)



UDMH

MMH



SO₂

NO₂

Figure 4. SERS Spectra of the Hazardous Gases of Interest.

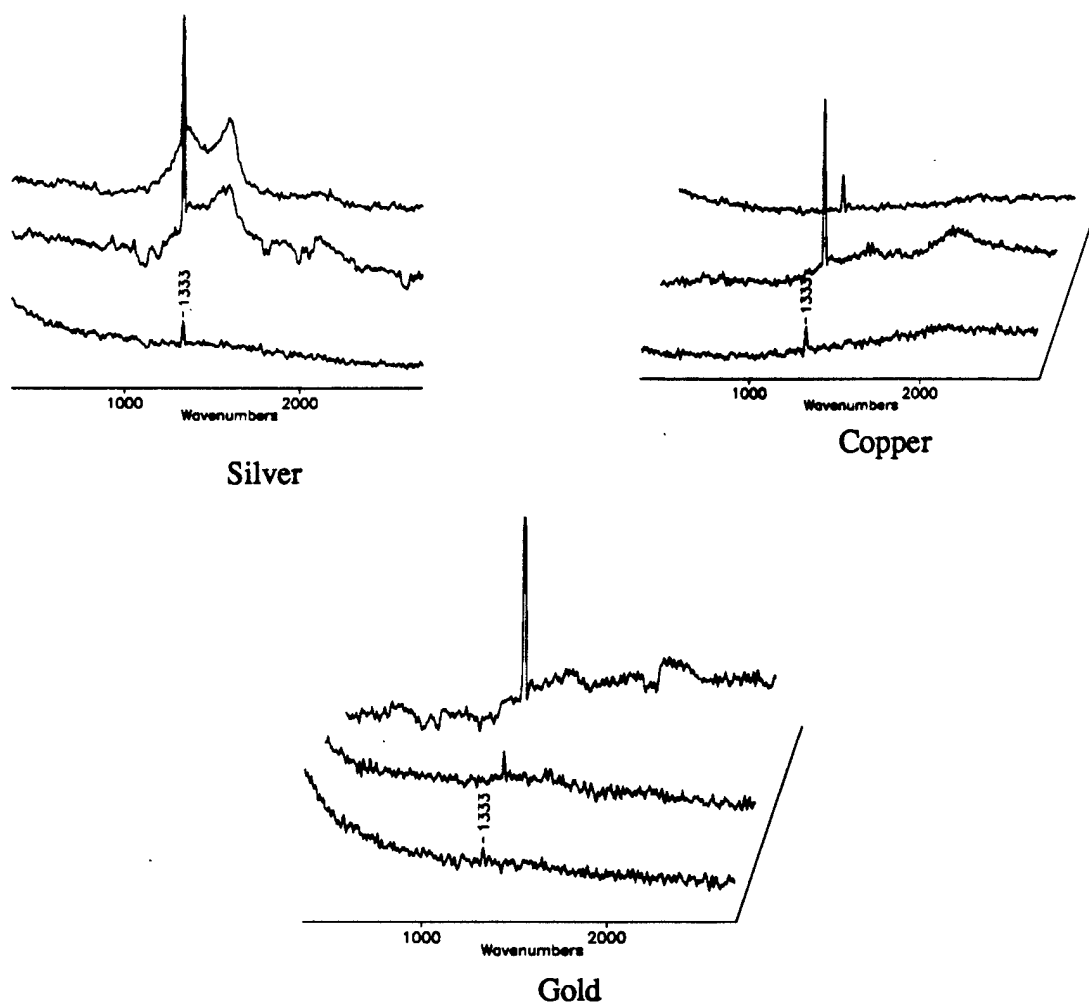


Figure 5. Raman Spectra of Diamond-Impregnated Ag, Cu and Au SERS Substrates. The Spectra are Displayed such that the Top Spectrum in each Trace is a Smooth Substrate, the Middle Spectrum Corresponds to the Roughened Substrate, and the Bottom Spectrum Corresponds to the Oxidized Substrate.

SERS spectra of the hazardous gases of interest were attempted using these diamond imbedded substrates. The SERS spectrum of NO_2 collected on a diamond-impregnated silver substrate is displayed in Figure 6. In this case, the electrode is not removed between the ambient air and NO_2 conditions and the expected constant intensity in the diamond band is observed.

Difficulties were encountered in obtaining reproducible SERS spectra of the hazardous gases when utilizing diamond-impregnated SERS substrates. One explanation could lie in surpassing a critical level of diamond present on the surface. Since diamond is an insulator, a large percentage present could curtail the charge transfer properties associated with SERS enhancement, as well as inhibit possible surface reactions. An equally plausible explanation is that the lack of reproducibility was not a function of the impregnated diamond but was inherent in the manufacturing process of the SERS substrates. The diamond-impregnated experiments were suspended until the question of reproducible SERS substrates could be adequately ascertained.

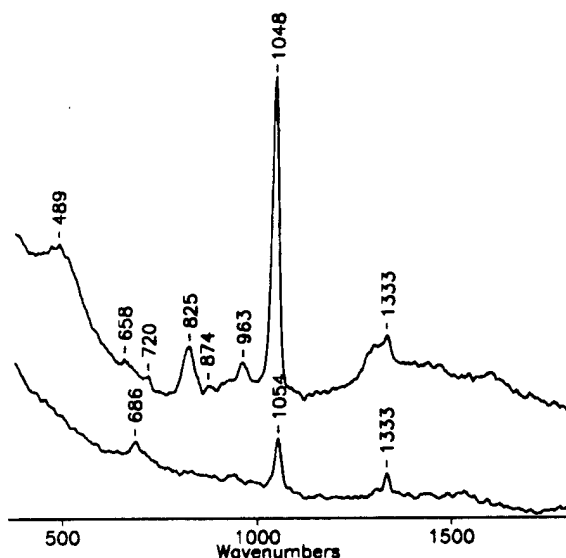


Figure 6. SERS Spectrum of a Diamond-impregnated Silver SERS Substrate in Ambient Air (Bottom) and in the Presence of NO_2 (Top).

D. EVALUATION OF A PHTHALOCYANINE OVERCOATING

Phthalocyanines undergo reversible reactions with numerous gases, including NO_2 and the hydrazines (Snow, 1984). Phthalocyanines have also been shown to undergo SERS enhancement on silver substrates (Jennings, 1984; Hayashi, 1985). We decided to pursue the following experiments where a thin layer of phthalocyanine was coated onto a silver substrate and then the coated substrate was placed in the presence of a hazardous gas. The hazardous gas reactions would then alter specific Raman bands in the phthalocyanine spectrum while leaving other bands unchanged. The phthalocyanine could effectively serve as the hazardous gas detection surface and the internal standard simultaneously.

Metal phthalocyanine surface layers are prepared by deposition of the phthalocyanine complexes from methylene chloride solutions onto roughened silver surfaces or by evaporation of the metal phthalocyanine complexes onto roughened silver surfaces. Figure 7 shows the SERS spectra of cobalt phthalocyanine (solution deposited) and lead phthalocyanine (vacuum deposited) on roughened silver substrates. The presence of the roughened silver underlayer results in an enhancement 20 times greater than for the standard Raman spectrum of the phthalocyanines.

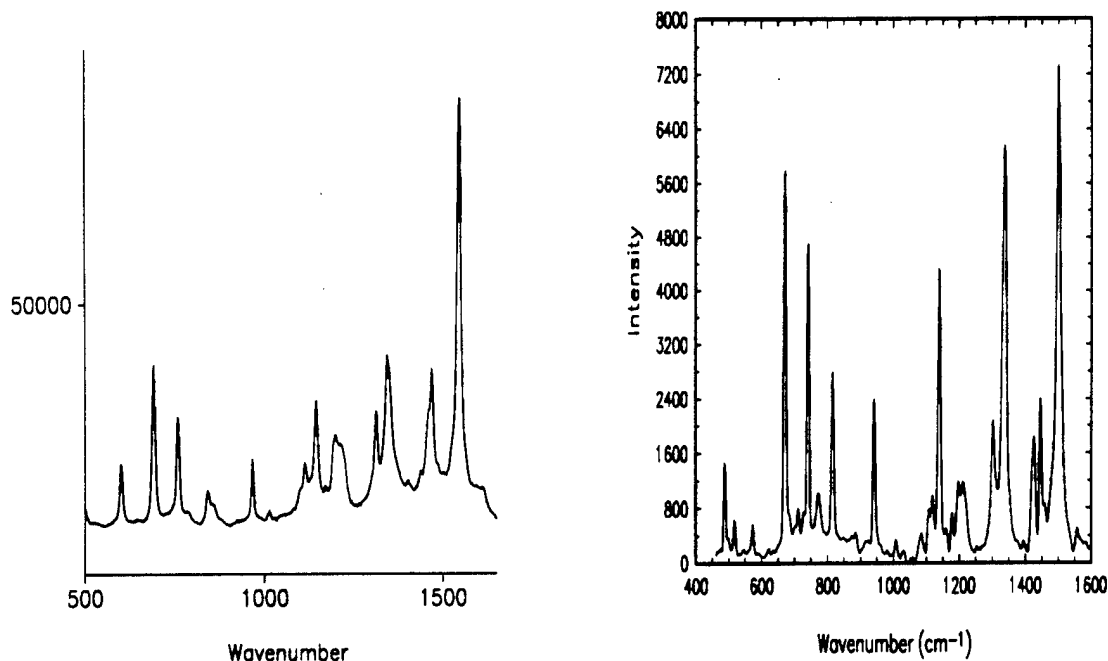


Figure 7. Left - SERS Spectrum of a Cobalt Phthalocyanine/Silver Substrate in Air. Right - SERS Spectrum of a Lead Phthalocyanine/Silver Substrate in Air. Each Spectrum was Collected using 50-mW of 676.4-nm Laser Radiation.

Initial SERS testing in the presence of hazardous gases produced no discernable change in the phthalocyanine spectrum. The lack of SERS enhancement for the hazardous gases indicated that the phthalocyanine layer was too thick and obscured the SERS enhancement from the silver underlayer. If the phthalocyanine layer was made too thin, then the phthalocyanine SERS intensity would be too weak. It was therefore necessary to evaluate the optimum phthalocyanine thickness.

Copper phthalocyanine was vacuum deposited onto a roughened silver substrate with deposition times of 1, 2, 3, 4, and 5 seconds. The SERS intensity of these surfaces was then determined using 676.4-nm laser radiation. A plot of the SERS spectra as a function of vacuum deposition times is shown in Figure 8. The SERS signal intensity was maximized with a deposition time of 2 to 4 seconds. With the current equipment, more precise determination of the optimum signal or control of the phthalocyanine thickness was not feasible.

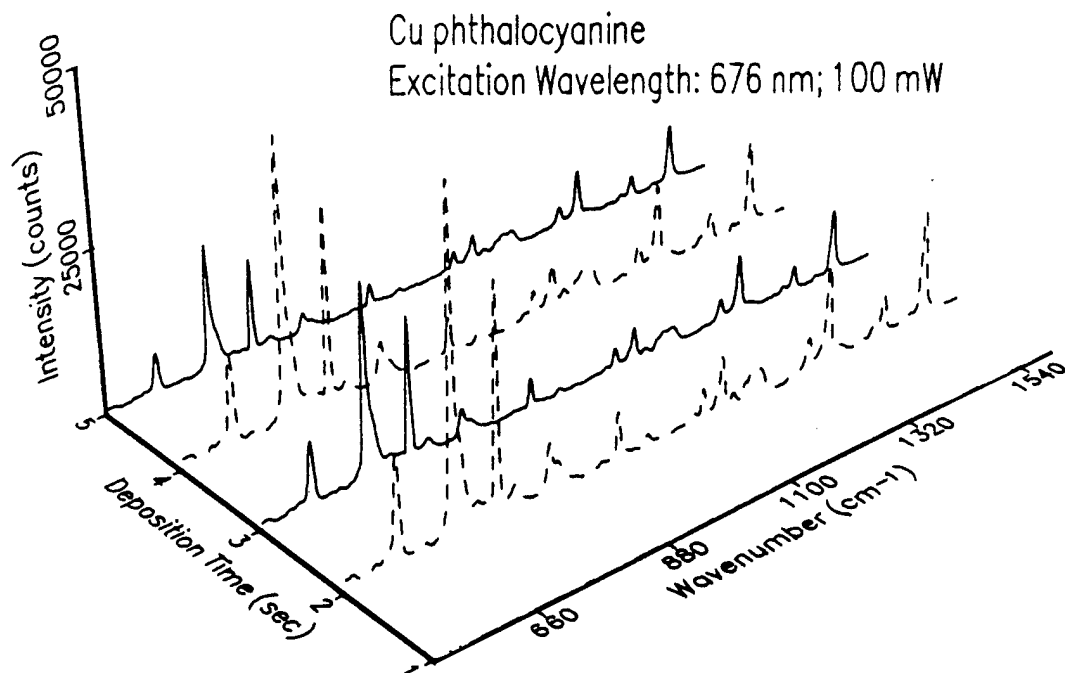


Figure 8. SERS Spectra of Copper Phthalocyanine/Silver Substrates Collected at Varying Vacuum Deposition Times.

With the phthalocyanine overcoating, there is no intrinsic reason for the SERS excitation profile to be the same. The SERS signal strengths for the copper phthalocyanine were collected at 676.4-nm and 514.5-nm. The SERS spectra are displayed in Figure 9. Different Raman bands show radically different enhancements as a function of the excitation wavelength. However, each wavelength exhibits strong SERS signals for the copper phthalocyanine.

Hazardous gases were allowed to flow across the face of the SERS substrates and spectra were collected. At an excitation wavelength of 514.5-nm, no changes were observed on the phthalocyanine/silver substrates at any thickness. However, exposure of the copper phthalocyanine/silver substrates to 50-ppm NO_2 results in an increase in the intensity of the peaks at 1105, 1144, 1165, and 1198- cm^{-1} when a 676.4-nm laser excitation source is employed. The intensity of these bands decrease when flushed with noncontaminated air, indicating that the reaction was reversible. The SERS spectra obtained on the 5 s vacuum-deposited substrate are shown in Figure 10. Although the thinner phthalocyanine layers also respond to NO_2 , the reversibility is much slower.

Testing with the other hazardous gases of interest yielded the same results. Therefore, although a useful internal standard is gained, compound specificity is lost. Since one of the key features of SERS is unique chemical identification, the phthalocyanine coatings do not appear to be an advantage to this program.

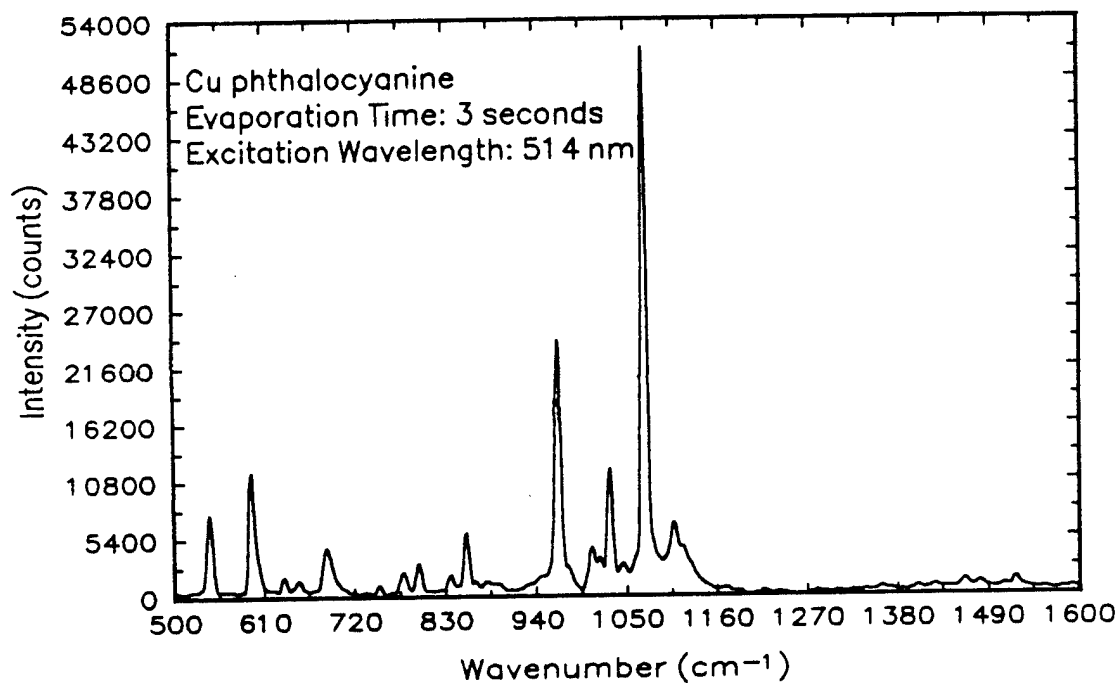
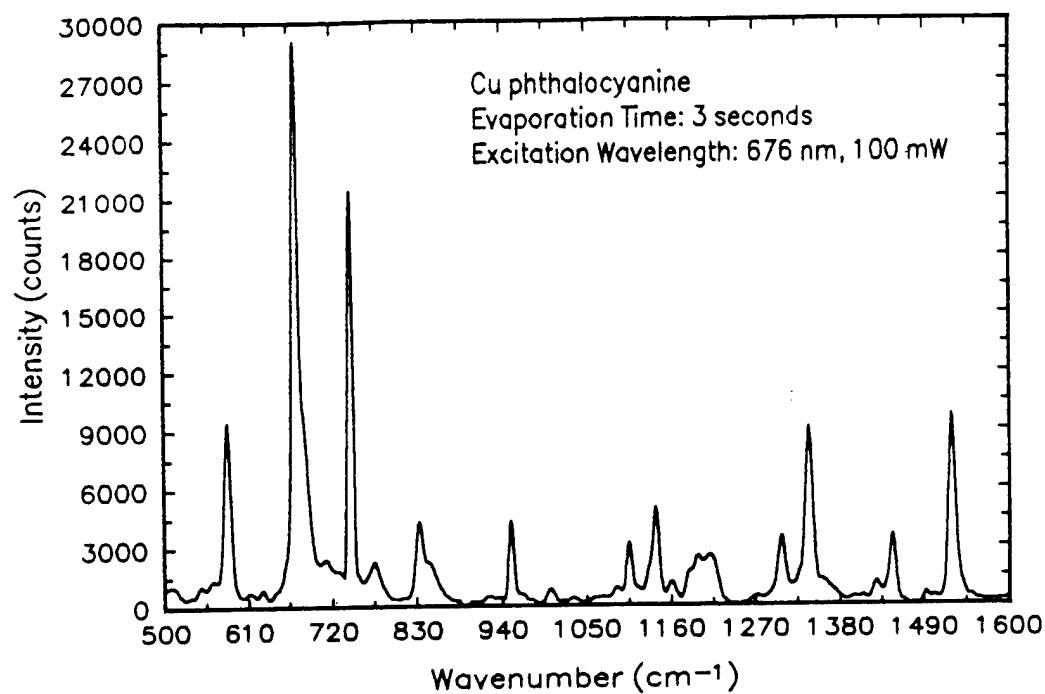


Figure 9. SERS Spectrum of a Cobalt Phthalocyanine/Silver Substrate in Air. Top - 100-mW of 676.4-nm Laser Radiation. Bottom - 50-mW of 514.5-nm Laser Radiation.

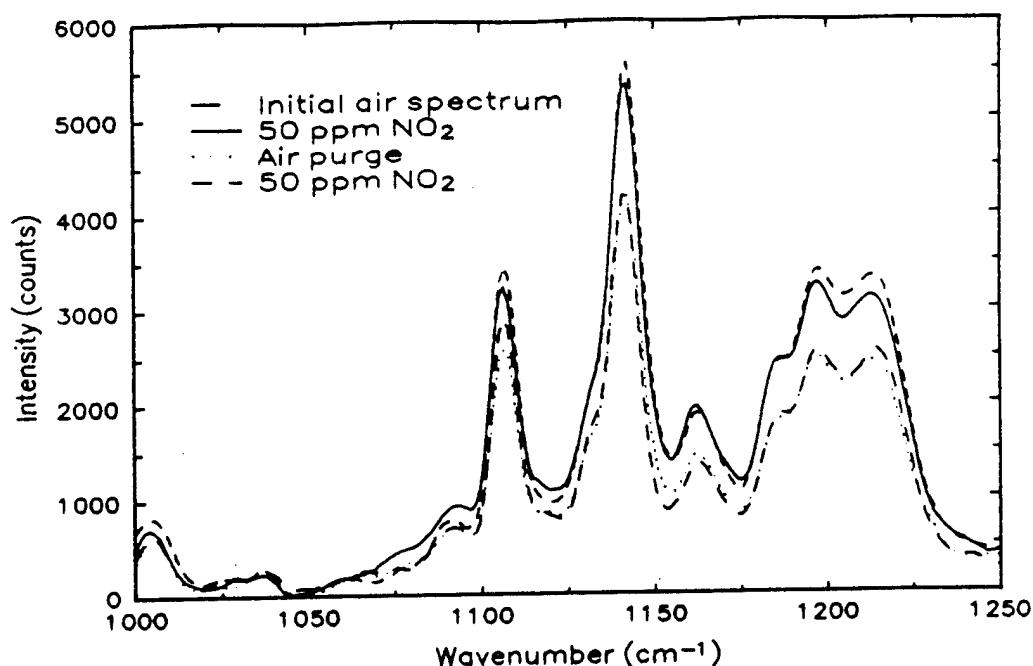


Figure 10. SERS Spectra of a Copper Phthalocyanine/Silver Substrate in Air, then 48-ppm NO₂, then Air, then 48-ppm NO₂.

E. VACUUM DEPOSITION VERSUS ELECTROCHEMICAL SUBSTRATES

The Phase I research program showed the feasibility of using biphasic SERS substrates prepared by vacuum deposition (sputtering and thermal evaporation) for hazardous gas detection. The determination of the suitability of vacuum deposition as a method of fabrication of substrates with a reproducible response was continued during the Phase II program. The first phase of the biphasic substrates consisted of a SERS active metal. The second phase, in intimate contact with the first, serves to interact with the gaseous species. The form of this interaction may be physisorption, chemisorption or direct chemical reaction. This second phase needs to be sufficiently thin and/or porous to bring the adsorbate or product close enough to the surface of the first layer to induce SERS enhancement.

The key factor in developing specific substrates for a SERS-based instrument for hazardous gases is the selection of the porous material that acts as an adsorbent and/or reactant for the molecular species to be detected. The second phase layer must interact with selected species present in the gaseous environment leading to their concentration and confinement onto that surface at positions near SERS active sites ($<200\text{\AA}$). Thus, both the chemistry and the morphology of the substrate must be considered.

Various oxide layers were prepared on deposited noble metal underlayers and SERS spectra of the resultant substrate in the presence of 10-ppm MMH were collected. The results of these tests are given in Table 1. Only a silver oxide layer appeared to be capable of reversibility and stability.

Once the silver oxide layer was determined to be the most useful oxide layer, the most appropriate method for application of the oxide to the base metal needed to be investigated. Three

options were a plasma oxidation, an electrochemical oxidation by maintaining a constant current (galvanostatic oxidation), or an electrochemical oxidation at a constant voltage (potentiostatic oxidation).

TABLE 1. POTENTIAL SUBSTRATES FOR THE DETECTION OF HYDRAZINES BY SERS

Substrate	Major MMH Bands (cm ⁻¹)	Concentration Dependent	Reversibility	Stability	Response Time	Preparation Method
AgO ₂ /Ag	1047, 995, 890	Yes	Reversible	Excellent	Rapid	Electrochemical Oxidation
AgO ₂ /Ag	980	Yes	Thermally Reversible	Moderate	Rapid	Sputtering
AgO ₂ /Au	980	Yes	Thermally Reversible	Moderate	Rapid	Sputtering
Al ₂ O ₃ /Ag	1047, 890	Yes	Reversible	Poor	Rapid	Evaporation
Al ₂ O ₃ /Au	1100, 470	Yes	Reversible	Poor	Rapid	Evaporation
IrO ₂ /Ir	981 ^a	No	Irreversible	N/A	Rapid	Electrochemical Oxidation
PbO ₂ /Pb	963, 783 ^a	No	Irreversible	N/A	Slow	Electrochemical Oxidation
WO ₃ /Ag	807, 600	No	Reversible	Good	Slow	Evaporation

Roughened silver surfaces were exposed to an oxygen plasma. The SERS spectrum of NO₂ on a plasma-oxidized silver surface is shown in Figure 11. In contrast to the SERS spectrum of the electrochemically prepared silver oxide surface, the SERS spectrum of the plasma prepared silver oxide surface shows a series of bands in the 600 to 1200-cm⁻¹ region. The plasma-oxidized Ag surfaces respond rapidly and reversibly to NO₂. In addition to a small 819 cm⁻¹ peak attributed to NO₂ on the electrochemical silver oxide surface (Figure 4), the plasma silver also shows a sharp, strong band at 1034-cm⁻¹. Upon exposure to air, both the 812 and 1034-cm⁻¹ bands disappear. SO₂ also responds reversibly to the plasma oxidized substrate. However, in sharp contrast to the electrochemical silver oxide substrates, the plasma-oxidized silver oxide substrates do not appear to be active for the detection of UDMH or MMH.

The two possible methods of electrochemical oxidation were then investigated. Galvanic oxidation using 40 mA/cm² was the standard procedure for preparation of the silver oxide surfaces. Galvanostatic oxidation produced substrates that reversibly responded to UDMH, MMH, and NO₂. Potentiostatic oxidation at -600 mV provided similar results. A comparison of the SERS spectrum of UDMH with each electrochemical process is displayed in Figure 12. Potentiostatic oxidation was chosen as the preferred method since spectral results appeared to be more reproducible.

SERS spectra could be obtained utilizing vacuum deposited metals or electrochemically roughened metals. During the Phase II program, no intrinsic advantage was established for vacuum deposition over electrochemical roughening. Although surface morphology should be more controlled during vacuum deposition leading to more reproducible SERS intensities, there was no

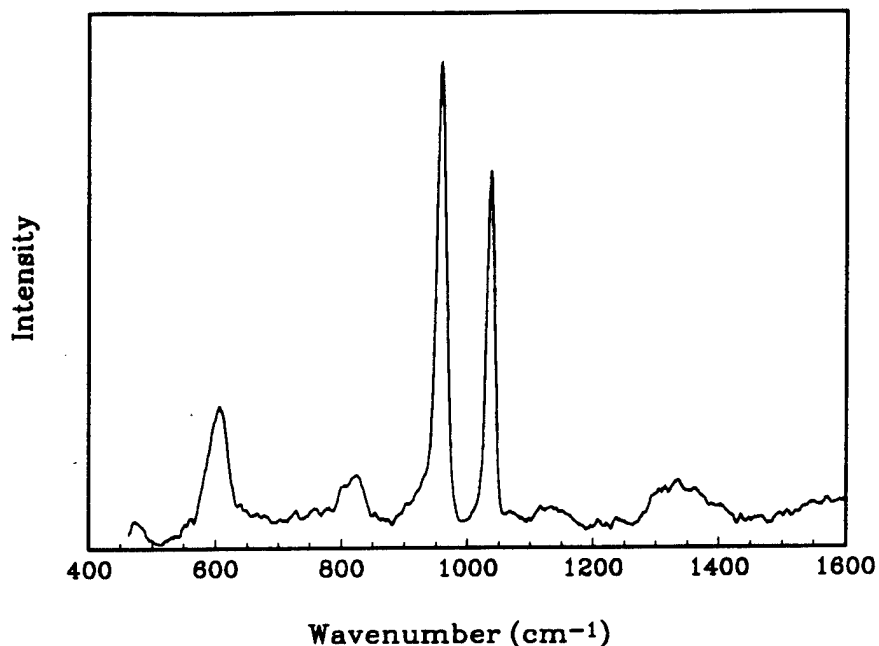


Figure 11. SERS Spectrum Obtained on a Plasma-Oxidized Silver Oxide Substrate in the Presence of 48-ppm NO_2 .

experimental confirmation. This is most likely due to contamination effects from a shared vacuum deposition unit. A dedicated sputterer would more than likely improve the reproducibility of the SERS substrates.

Since there is no apparent advantage to vacuum deposition, we decided to utilize electrochemically prepared electrodes for the remainder of the program. These electrodes are easier to prepare, more cost-effective, and renewable.

F. SERS REPRODUCIBILITY TESTING

Reproducibility has been used mainly to refer to signal consistency from one SERS substrate to another. This experiment was more concerned with signal reproducibility on a single reversible SERS substrate. Two electrochemically prepared silver oxide substrates were prepared and assembled in a custom optical cell designed to allow the parallel evaluation of long term performance and stability of each electrode. The optical cell design, a variation on the Figure 1 design in which the cell has been elongated to house two electrodes, allows the substrates to be simultaneously exposed to the same test gas. Any variations in the concentration of the test gas will be reflected in the response of both substrates. The substrates were periodically (every 1 to 5 days) exposed to a test gas containing 50-ppm MMH and the SERS spectra were recorded. When spectra were not being collected, the dual cell was purged with dry air. The substrates were exposed to the laser excitation source (676.4-nm) only while the SERS spectra were recorded.

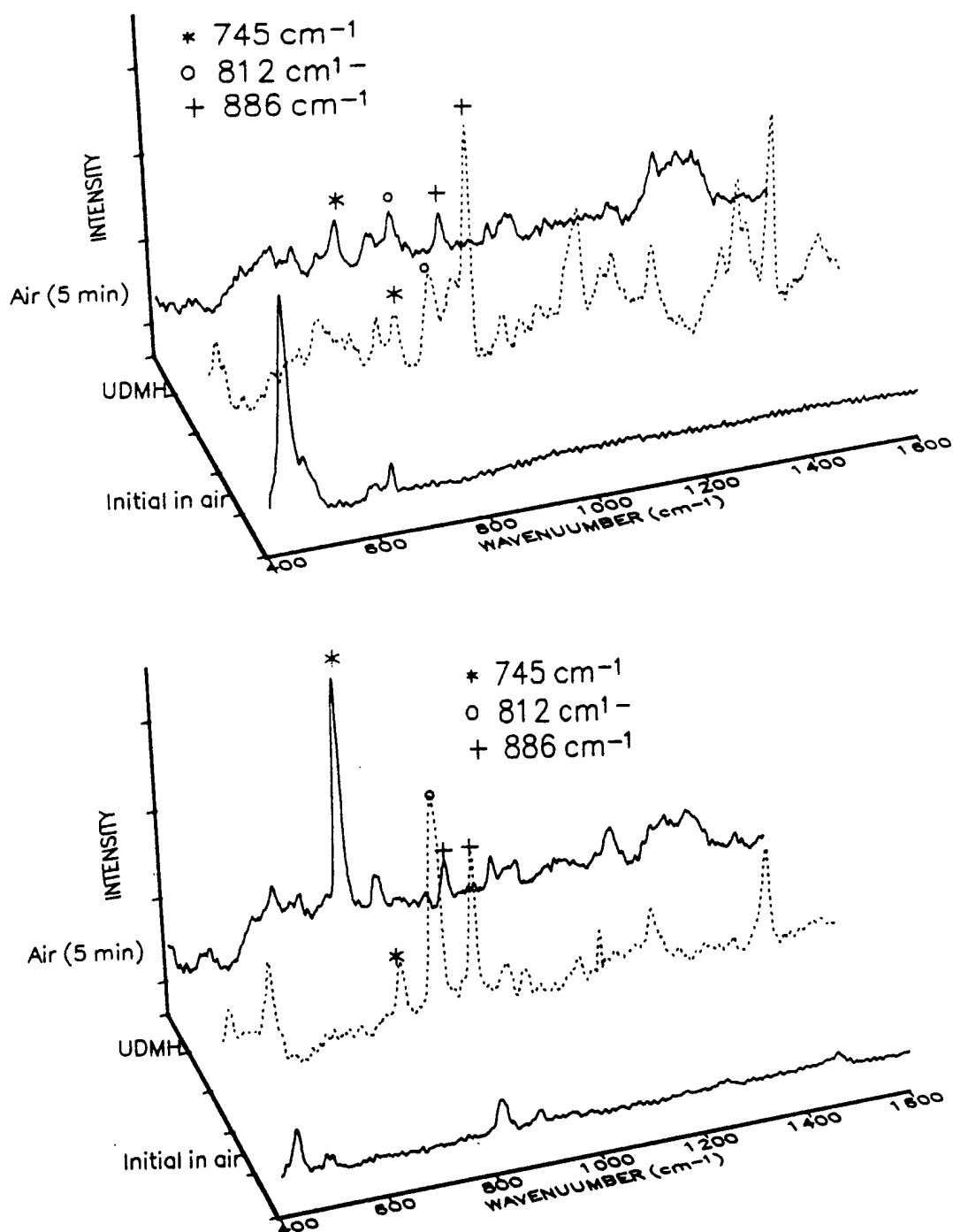


Figure 12. Top - SERS Spectra of UDMH on a Galvanostatically Prepared Silver Oxide Substrate: Initial Spectrum in Air, 30 Minute Exposure to 10-ppm UDMH and 5 Minute Exposure to Air. Bottom - SERS Spectra of UDMH on a Potentiostatically Prepared Silver Oxide Substrate: Initial Spectrum in Air, 30 Minute Exposure to 10-ppm UDMH and 5 Minute Exposure to Air. For each Spectrum, 125-mW of 676.4-nm Laser Light was Utilized.

The substrate response to the MMH test gas was determined by comparing the area of the 1047-cm^{-1} peak to the area of the 890-cm^{-1} peak. Figure 13 reveals the detected response obtained on the substrates after 80 days of measurement. There is a significant variation in the response; however, the variations are reflected in the response of both substrates indicating fluctuations in MMH concentration.

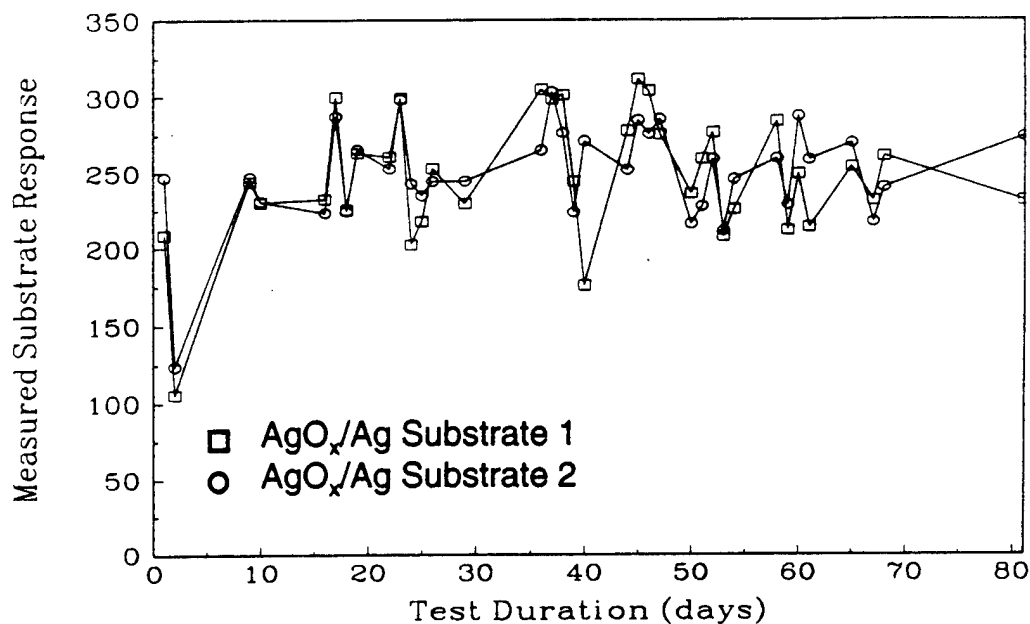


Figure 13. Measured Response of the Two Silver Oxide Substrates to 50-ppm MMH Recorded during the First 80 Days of Long Term Parallel Testing.

G. SERS WAVELENGTH AND SUBSTRATE TESTING

The experiments performed during the Phase I program never extended beyond 620-nm. It was necessary to determine the performance of the hazardous gases of interest further into the NIR excitation wavelengths. Experiments were performed employing the 514.5-nm laser line of the argon laser as well as the 647-nm and 752.5-nm laser lines of the krypton laser. Laser powers ranged from 25-90-mW. The SO_2 concentration was always 48-ppm. A 48-ppm NO_2 concentration was also employed. In addition, zinc metal was allowed to react with concentrated HNO_3 in a sealed vial to produce a concentrated NO_2 gas into which the electrodes could also be placed.

Representative SO_2 spectra at each of the laser wavelengths is presented in Figure 14. At all three wavelengths, a characteristic spectrum which can be assigned to the presence of SO_2 was detected. At 514.5-nm, the 960-cm^{-1} band dominates whereas the broad 925-cm^{-1} band is the main feature at 647 and 752.5-nm with the 960-cm^{-1} band being nothing more than a weak shoulder. The 960-cm^{-1} feature corresponds to surface adsorption of an SO_4^{2-} species whereas the broad shoulder and the 615-cm^{-1} band correspond to SO_3^{2-} (Dorain, 1981). From these results, SO_2 may be detected throughout the wavelength region of interest.

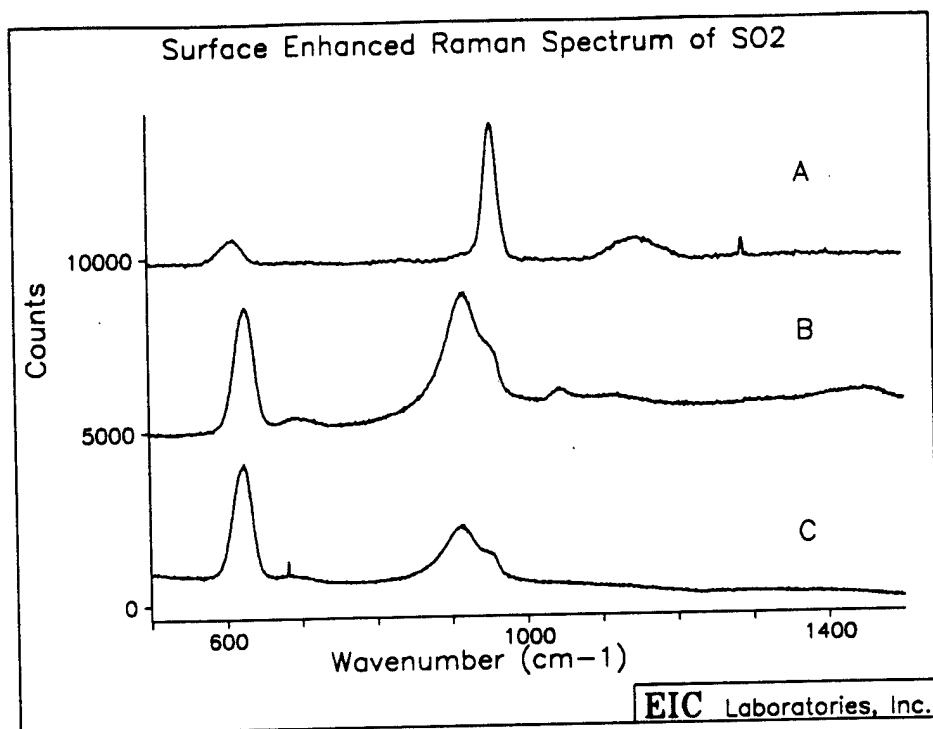


Figure 14. The SERS Spectrum of 48-ppm SO_2 at a) 514.5-nm, b) 647-nm, and c) 752.5-nm.

There are certain prerequisites for the detection of SO_2 using SERS. The silver electrodes had to be roughened by electrochemical cycling with NaNO_3 or by electrochemically cycling with KCl and removing the electrode after several minutes at a negative potential. Immediate removal of the electrode from KCl roughening at a negative potential did not appear to produce a SERS active substrate. This is most likely due to the fact that AgCl precipitated onto the electrode surface changing surface morphology in a manner which could not induce the SO_2 to react with the surface.

Electrochemical roughening was sufficient for detection of SERS spectra of the SO_3^{2-} species. However, if after roughening, the electrodes were oxidized in KOH to produce a biphasic SERS substrate the spectral features improved. In addition, gaseous oxygen was necessary for appearance of the SO_4^{2-} species and increased the size of the SO_3^{2-} spectral features. Oxygen in ambient air appears to be more than sufficient to initiate the reaction. Finally, the laser needs to be present for the reaction to occur. This is a thermal effect since the reaction occurs at several wavelengths.

SERS spectra for NO_2 on silver electrodes are presented in Figure 15. NO_2 at 48-ppm was not detectable at 514.5 nm. Concentrated NO_2 was detectable at 514.5 nm on electrodes that had been electrochemically roughened in NaNO_3 but not oxidized to the biphasic SERS substrate. In contrast, 48-ppm concentrations of NO_2 were detectable at 647 and 752.5-nm when the biphasic SERS substrate was employed. NO_2 did not appear to be affected by the presence of oxygen. The presence of the laser is necessary for the reaction to occur.

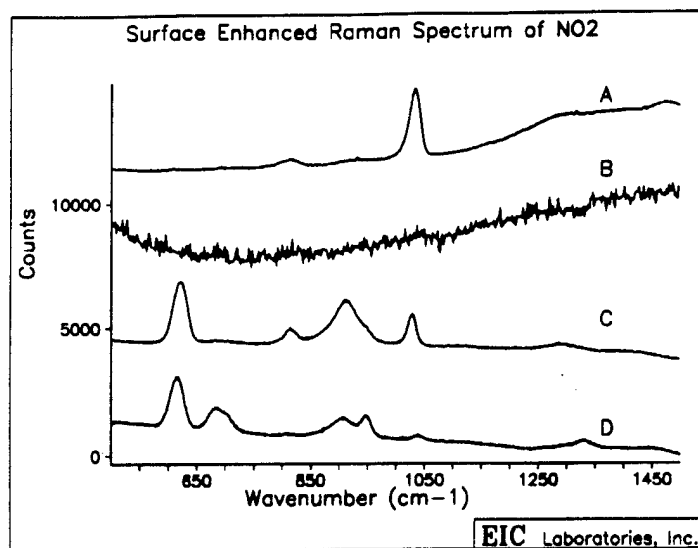


Figure 15. The SERS Spectrum of NO₂ at a) Concentrated Vapor using 514.5-nm Light, b) 48-ppm using 514.5-nm Light, c) 48-ppm using 647-nm Light, and d) 48-ppm using 752.5-nm Light.

Both thin silver wire (1-mm dia.) and large silver disks (6-mm dia.) were utilized as electrodes for these studies. Both gave reproducible results. For the prototype unit, the large silver disks were employed to insure proper alignment of the laser onto the silver surface.

Similar tests for UDMH and MMH demonstrated a similar preference to less energetic wavelengths. The results of these experiments verify that diode laser wavelengths (670-700-nm, 770-800-nm) can be utilized in the prototype instrument. At less energetic wavelengths, copper has shown greater SERS enhancement in aqueous solutions than the corresponding silver substrates. Tests were performed to determine the suitability of copper, copper oxide/copper, gold, and gold oxide/gold electrodes to act as SERS substrates for the hazardous gases of interest. Although some SERS enhancement was detected, no substrate was found to have greater sensitivity or reproducibility than the silver or silver oxide/silver substrates.

SECTION III

FABRICATION OF A PROTOTYPE SERS INSTRUMENT

A. DIODE LASER EVALUATION

Initial diode laser investigations centered around the Toshiba TOLD-9140 model. This diode laser could provide 25-mW of power in the 690-nm wavelength range. Diode laser power and wavelength of operation depend on the input current and the temperature of the diode laser head. Eight Toshiba TOLD-9140 diode lasers were tested during this program. All data was collected by launching the diode laser line into a fiber connected to a spectrograph. The spectral information collected from the CCD camera attached to the spectrograph was monitored for saturation effects. Neutral density filters were placed between the laser and the fiber, if needed, to prevent signal saturation.

A lifetime test was performed where one of the diode lasers was run continuously at its maximum current limit continuously. It was found that the diode laser could operate for over 1400 hours with no degradation of laser quality. However, continuous monitoring of the laser line revealed that, although the power characteristics were satisfactory, the laser wavelength was not stable.

Wavelength shifting of the laser line will, at the very least, lead to an unacceptable broadening of the Raman bands. The presence of multiple laser lines, or a continuously changing laser line, prohibits the utilization of these lasers as Raman sources since accurate assignment of Raman bands will be impossible.

Several other laser sources were tested. One of the more promising set of lasers was obtained from Spectra Diode Laboratories. These lasers, which operated at wavelengths between 775 and 810-nm were capable of attaining 100-mW power levels. In addition, the thermoelectric cooler was in the diode laser head to circumvent any problems that might occur due to changes in the ambient temperature. However, every laser tested showed some degree of wavelength instability.

Further investigation of the problem indicated that the position of the optical fiber or a standard optic immediately in the optic train after the diode laser varied the degree of laser instability. Subsequent testing confirmed that optical backreflections were entering the diode laser cavity and destabilizing the diode laser. To compensate for this optical feedback, the Spectra Diode Laboratories diode laser was equipped with an optical isolator (Optics for Research Model 10-DNM-FLB-TO3-775-F). The Spectra Diode Laboratories diode laser showed improved laser stability. There did appear to be minute laser wavelength changes which appeared to be related to the laboratory temperature.

Since laser instability was shown to be an optical feedback problem, the Toshiba TOLD-9140 diode lasers could probably be useful when coupled to an optical isolator. However, power differences between the Toshiba and the Spectra Diode Laboratories diode laser swayed the decision to the latter as the prototype laser.

B. FABRICATION AND EVALUATION OF THE PROTOTYPE ECHELLE SPECTROGRAPH

One of the major requirements of a Raman spectrometer is high resolution. To fulfill this requirement, normal dispersive spectrographs incorporate a combination of long focal lengths, multiple dispersive elements, and scanning mechanisms. These units are usually very large and somewhat complex. Our previous Phase I results established the feasibility of using compact spectrographs while still allowing for the identification and quantification in the region of 200 to 4000-cm⁻¹ from the excitation line.

Most commercially available spectrographs suffer from the problem of resolution vs. range. These spectrographs are designed to disperse the spectrum onto a 1-inch focal plane. One inch is selected because it is the common size of most diode array detectors. For Raman spectroscopy, one inch is the largest size diode array detector that is available. The optical constraints of the typical spectrograph dictate that the system either has high resolution (required for Raman) and a limited range (approx. 1000-cm⁻¹) or low resolution and an extended range (200 to 4000-cm⁻¹).

The limited spectral range in the high resolution system means that to obtain the complete Raman spectrum the spectrograph grating position will have to be shifted four times. This is a prohibitive situation, particularly for a field instrument to be operated by nonspecialists. An alternative type of compact spectrometer which can provide high resolution and a large dynamic range is an echelle spectrograph. The echelle system is designed to achieve a high degree of dispersion in a very compact size while obtaining the entire spectral range with a resolution of ~1-cm⁻¹ without the need for moving or shifting the grating or any other optical components. The design incorporates a commercially available 52.65 g/mm echelle grating (Milton Roy 35-15-415) operated in the Littrow configuration at its blaze angle of 63.4°, in order to achieve maximum efficiency. The diffracted orders incorporating the desired energy range are obtained using the grating equation:

$$m\lambda = a(\sin \alpha \pm \sin \beta) \quad (1)$$

Here, m is the diffraction order, a is the groove separation, α is the angle of incidence with respect to the grating normal, and β is the angle of diffraction. The grating divides the 4000-cm⁻¹ interval (the range for a complete Raman spectrum) into 14 orders. Using 775-nm laser light as the excitation source, the relevant echelle orders are orders 44-30. For echelle gratings, the free spectral range (F) in each order is given by

$$m = \nu/F \quad (2)$$

The calculated spectral range of our system is thus approximately 295-cm⁻¹/order.

The length of the spectral range of each echelle order is directly proportional to the focal length of the lens and the angle at which the incident light impinges upon the lens. The optical equation is given as:

$$I = 2(f \tan \alpha) \quad (3)$$

where f is the focal length of the lens and α is the angle of incidence. Light of higher energy is dispersed at less severe angles than the low energy light. As a result, the length of each echelle order increases as the wavelength decreases. If a 150-mm focal length lens is employed in the prototype unit, then the length of the spectral range of echelle order 44 is 14.58-mm while the length of echelle order 31 would be 20.72-mm. This was an appropriate focal length to utilize for the prototype unit since the CCD chip is only 26-mm long.

Since the spectral range in each order is constant ($295\text{-cm}^{-1}/\text{order}$) while the length of the spectral range is changing in each echelle order, the resolution is not constant. The theoretical limit to resolution would be the range divided against the number of CCD pixels encompassed within the length of the free spectral range. For echelle order 44, 648 pixels are utilized and the maximum theoretical resolution would be $0.45\text{-cm}^{-1}/\text{pixel}$. For echelle order 31, 921 pixels are utilized and the maximum theoretical resolution would be $0.32\text{-cm}^{-1}/\text{pixel}$. Therefore, since a CCD pixel element is $22.5\text{-}\mu\text{m}$ wide, 1-cm^{-1} resolution could be achieved on all desired echelle orders if a $25\text{-}\mu\text{m}$ slit or input fiber was utilized. Throughput considerations make a $100\text{-}\mu\text{m}$ input fiber more desirable. This reasonable compromise provides a resolution ranging between $1.5\text{-}2.25\text{-cm}^{-1}$.

Practical considerations will not allow the entire range from $0\text{-}4000\text{-cm}^{-1}$ to be collected. The CCD camera cannot detect light emitted at wavelengths greater than approximately $1.03\text{-}\mu\text{m}$. This puts an upper limit on spectral collection when employing a 775-nm diode laser in the 3200-cm^{-1} range. No spectral information can be obtained from echelle orders 31 and 30. In addition, if the laser line were allowed to reach the CCD camera unimpeded, the laser line signal would saturate the detector and invalidate spectral collection. Therefore, edge filters must be employed to remove scattered laser light while allowing scattered Raman signal to pass into the echelle spectrograph. The edge filters employed in this unit do not allow collection of any light from $0\text{-}200\text{-cm}^{-1}$. Therefore, the practical spectral range is from $200\text{-}3200\text{-cm}^{-1}$. These limitations are not a result of the echelle spectrograph and would have to be considered on any spectrograph.

A schematic of the prototype echelle unit is shown in Figure 16. A $100\text{-}\mu\text{m}$ fiber-optic (1) is mounted to the inner wall of the echelle spectrograph and transfers the light to the 150-mm focal length lens (3) which collimates the collected light. In between the fiber-optic and the lens is an electronic shutter (2) which allows the Raman signals to enter into the echelle when desired. The collimated light is then dispersed into collimated wavelength packets by a set of prisms (4) before being dispersed into different echelle orders by the echelle grating (5). The two-dimensional array of collimated light is then focused by a camera lens (6) onto the CCD camera face (7).

The lenses employed in the prototype instrument were commercially available (Navitar) 75-mm lenses. Extenders (2x, Fujinon) were attached to each camera lens to attain the desired 150-mm focal length. The system was aligned by following the 752.5-nm krypton laser line through the optical elements. The prism mount was designed so that the prisms would fit in at the specified design angle only. The echelle grating mount was designed to allow for fine adjustment of the in-plane and out-of-plane grating angles. The grating angle was adjusted until the 752.5-nm laser line was near the top of the CCD camera. The spot size observed was minimized by adjustment of the camera lens focal length. A $100\text{-}\mu\text{m}$ fiber-optic employed as the entrance slit will result in a 5-pixel x 5-pixel image at the CCD camera for the unit magnification echelle. The laser line image with expected spot size is shown in Figure 17.

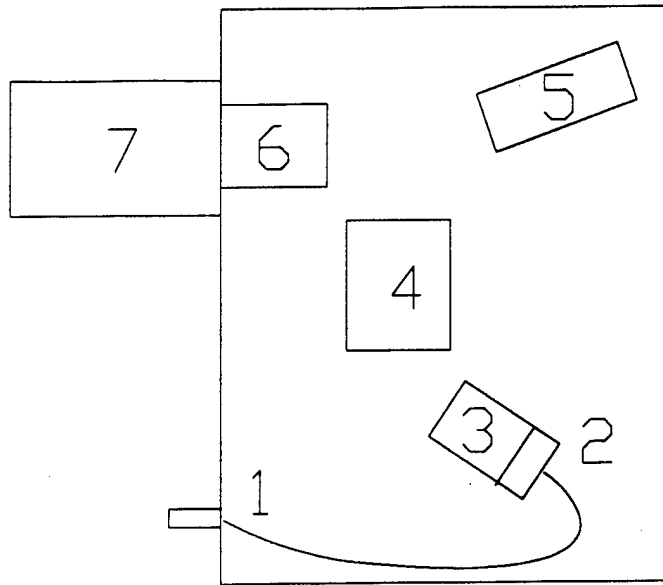


Figure 16. Schematic of the Prototype Echelle Spectrograph.

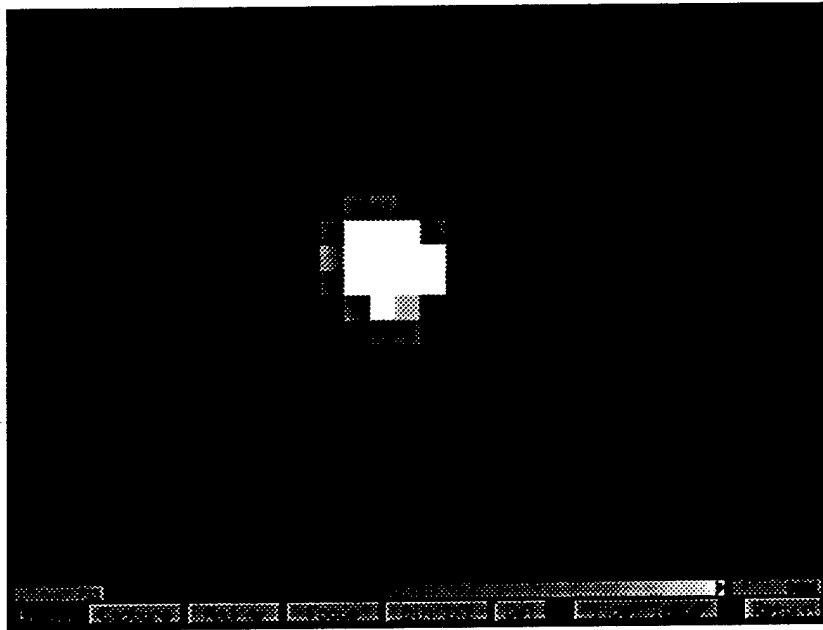


Figure 17. Spot Size on the Echelle Spectrograph.

Once satisfied with the image quality, a white light spectrum was collected. The white light spectrum served two purposes during prototype evaluation. First, it identified the regions on the CCD camera where the echelle orders were active. Second, the image of the white lines on the chip served as an aid in the rotational alignment of the CCD camera onto the echelle spectrograph. When

the white light lines appeared to be parallel to the long edges of the CCD camera chip, as visualized with the CCD9000 software, the CCD camera was correctly aligned. The white light spectrum is presented in Figure 18.

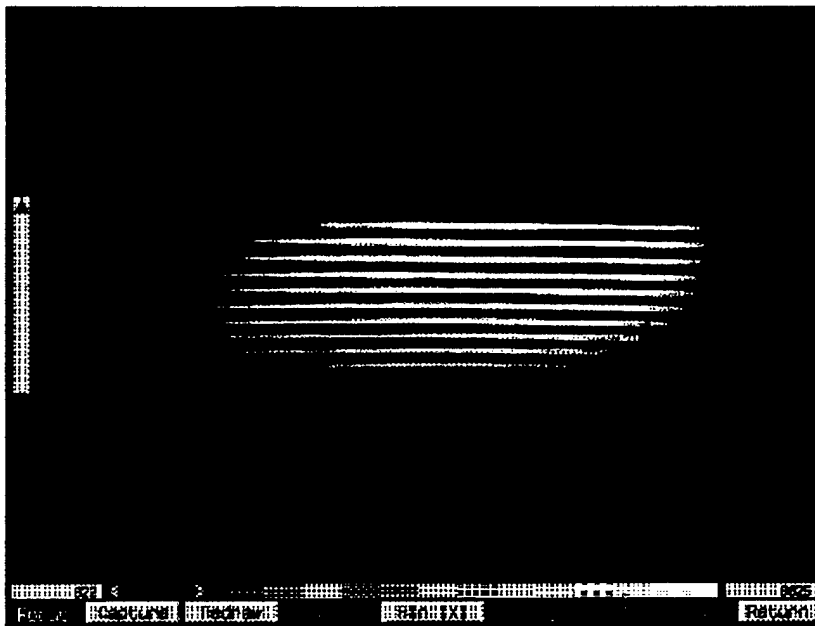


Figure 18. Image of the White Light Spectrum on the Prototype Echelle Spectrograph.

The white light spectrum presented us with an inconsistency. As seen in Figure 18, the white light spectrum lines are kept within a circular trace on the CCD camera chip. This is an indication of the clear aperture limit of the camera. From calculations presented earlier, the longest free spectral range of a desirable echelle order is 20.72-mm on a 26-mm chip. A quick glance at Figure 18 reveals that the clear aperture limit of the camera will not allow spectral collection across 80% of the CCD chip. Therefore, information would probably be lost at the ends of the longer free spectral ranges, leaving gaps in the Raman spectral information.

Collection of Raman spectra verified this information loss. Presentation of Raman spectra with missing Raman bands was unacceptable. Investigation of the camera limitations revealed that the 2x focal length extender was responsible for the reduction of useful clear aperture. One option would be to custom design a NIR lens with the 150-mm focal length that would have the necessary clear aperture. This is the best option and is being pursued by EIC Laboratories. However, the time required for custom lens fabrication made Phase II prototype installation unfeasible.

Another method by which to counter the extender limit is to remove the 2x extender on the 75-mm focusing lens at the CCD. The length of the free spectral range will decrease by a factor of 2, as shown by Equation (3). This will lead to a doubling of the resolution limit since the number of pixels employed has decreased. If the collimating lens maintains its 150-mm focal length, the echelle no longer has unit magnification but is instead demagnifying the spot by a factor of 2. Therefore, the utilization of a smaller CCD area can be compensated for by creating a demagnifying

spectrograph. An additional advantage gained from this is improved throughput, since the Raman intensity is shared between fewer pixels and the throughput losses associated with the 2x extender have been removed.

This method was employed and the expected demagnification was observed. Operation as a demagnification spectrograph allowed collection of a complete Raman spectrum. The throughput levels appeared to be satisfactory. The next issue to be addressed was the fabrication of an appropriate Raman probe and SERS insert.

C. FABRICATION AND EVALUATION OF THE SERS INSERT

Ideally, the fiber-optic Raman probe should have been fabricated and then the SERS insert installed and tested. However, delays in the optimization and choice of a laser source did not allow us the luxury of waiting for the correct fiber-optic Raman probe to be fabricated before construction and testing of the SERS insert. Several fiber-optic Raman probes had been previously fabricated at 514.5-nm. We decided to fabricate the SERS insert and test it with the 514.5-nm Raman probe using SO₂.

The SERS inserts can be attached to the front face of the Raman probe. These inserts hold the large silver electrodes and restrain the front face of the electrode so that it is at the focal point of the Raman probe. The insert attached to the Raman probe is drawn schematically in Figure 19. This insert is constructed of Teflon®, which has greater resistance to hydrazine attack than conventional gas tubing. The insert attaches to the Raman probe via set screws and the electrode is held into the insert by set screws. The depth of the Raman probe and electrode into the insert are controlled through the use of mechanical stops. The electrode is centered with respect to the focussing lens and not with respect to the cell body to minimize alignment mishaps. Threaded holes allow gas lines to be attached in the laboratory. Removal of the Teflon® elbow fittings will allow ambient air at a deployment site to flow across the electrode.

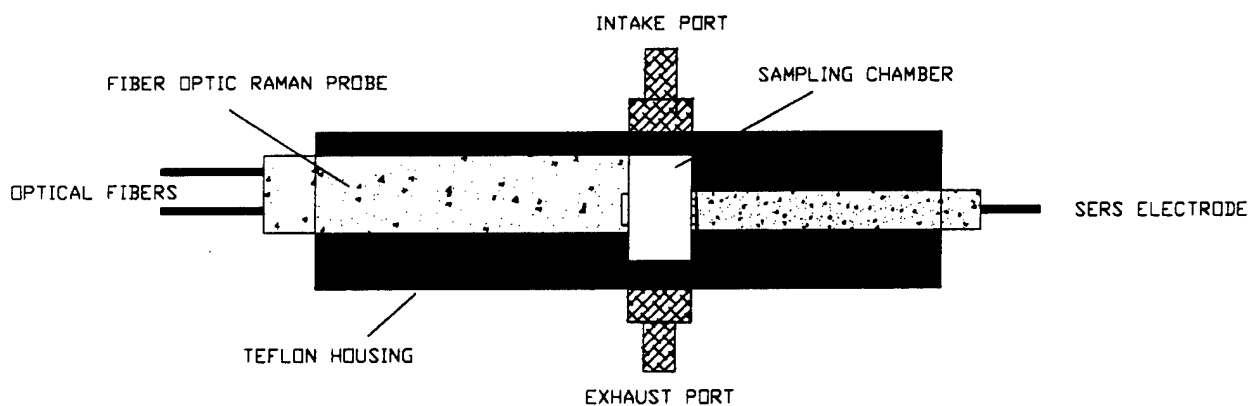


Figure 19. Schematic of the SERS Insert Coupled to the Fiber-Optic Raman Probe.

Preliminary testing of the fiber-optic SERS probe utilized SO_2 as the gaseous species since SO_2 had shown the greatest affinity for silver when 514.5-nm laser light was employed in earlier wavelength studies. As in previous experiments, the presence of oxygen is necessary for the SO_2 to react with the surface. The initial experiments utilized 50-ppm SO_2 and are presented in Figure 20.

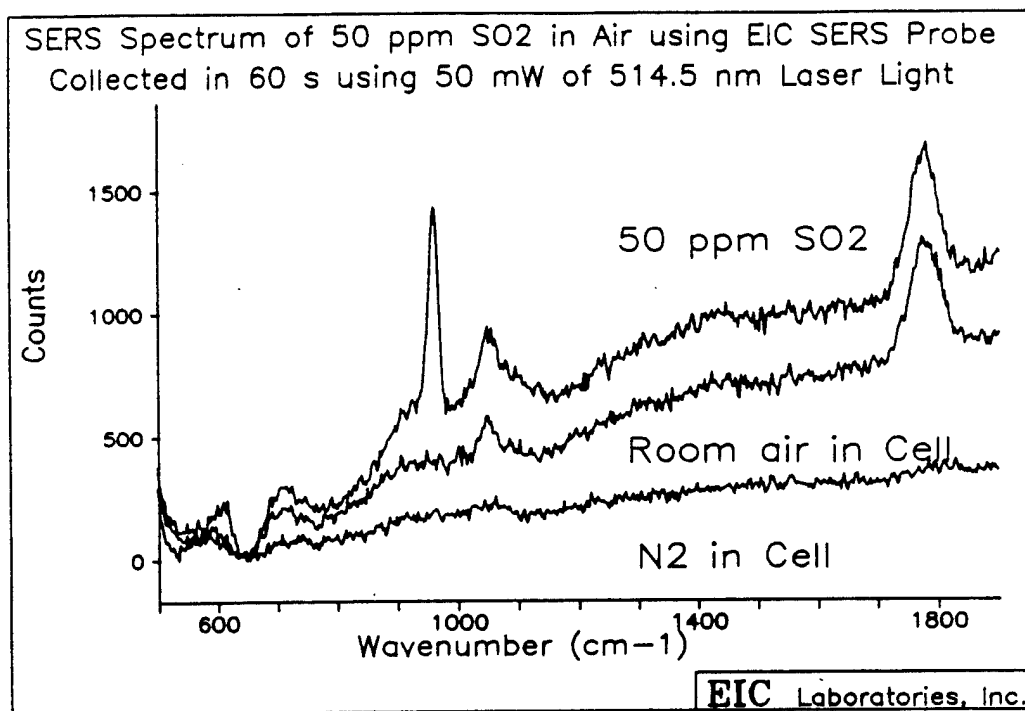


Figure 20. Fiber-Optic SERS Spectrum of 48-ppm SO_2 Collected at 514.5-nm.

As more familiarity with the SERS insert was acquired, better signal levels were obtained. This is demonstrated in Figure 21 where the SO_2 concentration has been diluted to 5-ppm. The signal-to-noise level for this spectrum is very good, indicating that 100-ppb levels or lower of SO_2 would be detectable. These experiments clearly demonstrated that the SERS insert design was correct and was used without further modification for the prototype system.

D. FABRICATION AND EVALUATION OF 775 NM FIBER-OPTIC RAMAN PROBE

With the determination of the prototype wavelength, the fiber-optic Raman probe could be fabricated. The EIC filtered probe design, shown in Figure 22, utilized the same lens for delivery of the excitation source to the sample and collection of the Raman signal. This is also called 180° backscattering. The Raman signal is separated from the scattered laser light within the Raman probe through the efficient use of a dichroic filter followed by a dielectric edge filter. The filters were specifically designed to work most efficiently for a diode laser operating at 775-nm. This probe is easier to align and has a higher signal throughput since there is total overlap between the excitation and collection cones.

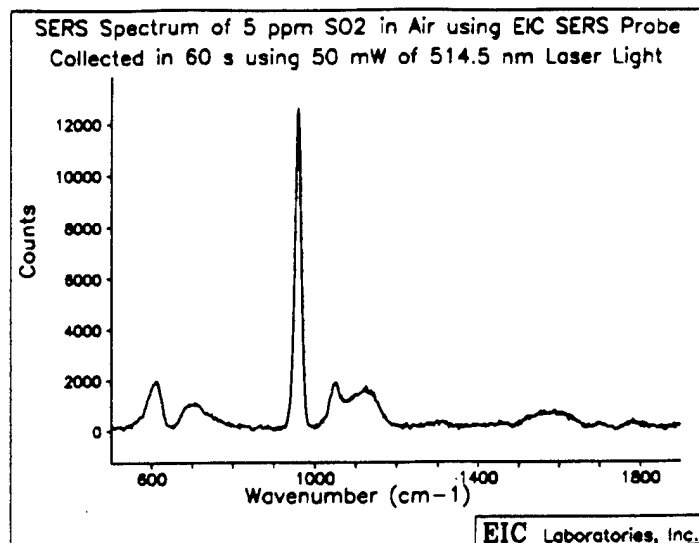


Figure 21. Fiber-Optic SERS Spectrum of 5-ppm SO₂ Collected at 514.5-nm.

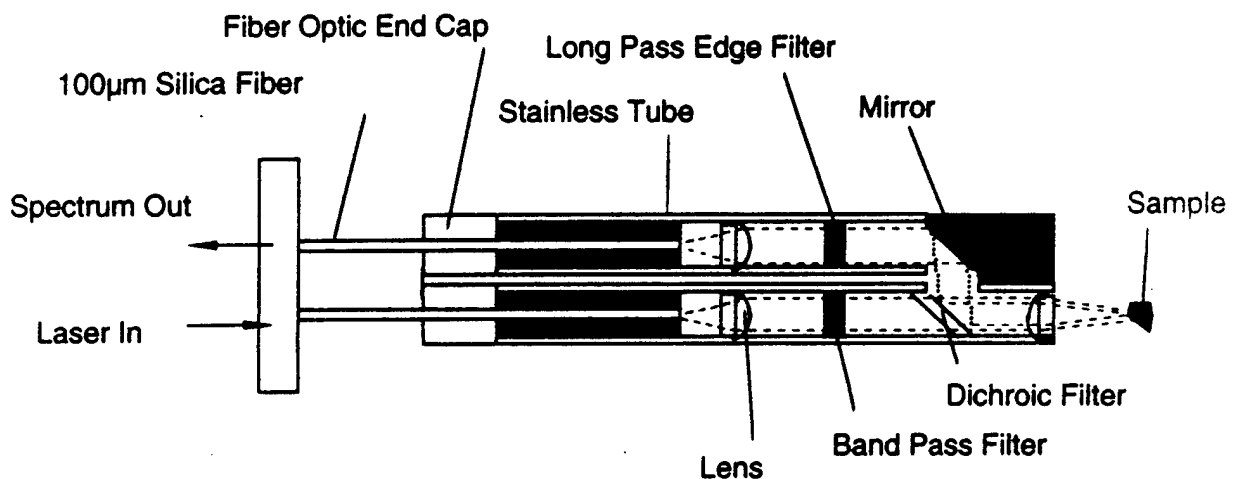


Figure 22. Schematic of the Fiber-Optic Raman Probe.

Alignment of the probe is easily accomplished for the backscattering probe. The 775-nm laser is pumped in the laser fiber while the 514.5-nm line of the argon laser is passed through the collection train. The two laser trains are visually observed at the lens surface, near the focal point, and at some point beyond the focal point. When the two optical trains are in the Raman body at the proper orientation, the observed laser beams will be superimposed at all points in space.

Probe throughput was determined by measuring laser power before entering the fiber and the laser power exiting the lens. The throughput for the 775-nm probe was 55%. This value is acceptable since the dichroic filter employed has a maximum transmittance of 70% by itself and 10% is expected to be lost in the coupling of the fiber to the laser. Finally, the fiber-optic Raman probe was used to collect Raman spectra of some standard compounds using the dye laser set to 775-nm to emulate the diode laser. The spectra obtained indicated the fiber-optic Raman probe was functioning properly.

Once satisfied with the 775-nm Raman probe, the SERS insert was attached to the Raman probe and SERS spectra of the hazardous gases of interest were collected. The SERS spectrum of 14-ppm UDMH collected with the probe is shown in Figure 23. The SERS spectra collected indicated that the fiber-optic Raman probe with SERS insert was acceptable for the completion of the prototype.

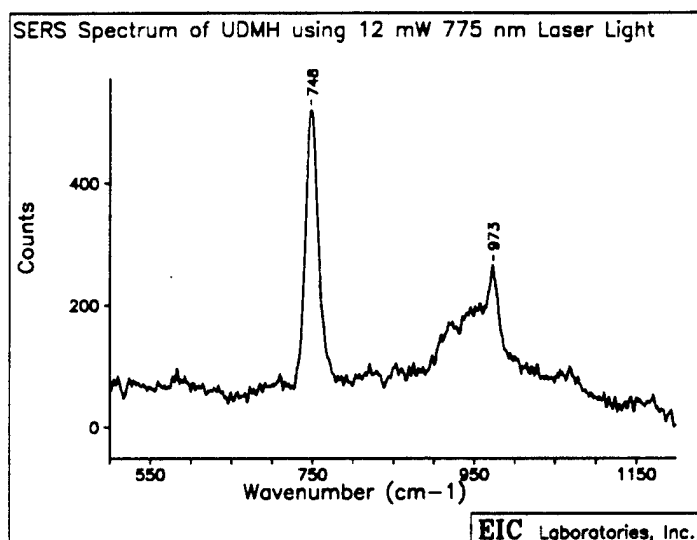


Figure 23. SERS Spectrum of 14-ppm UDMH on a Silver Substrate at 775-nm.

All the components for the prototype had been designed, evaluated, modified and satisfactorily evaluated. All that remained was integration of the components into a single portable unit.

SECTION IV

EVALUATION OF THE PROTOTYPE INSTRUMENT

The entire prototype was fabricated on a 32" x 24" metal plate. The echelle spectrograph was mounted onto the plate, as was the diode laser. Rubber gaskets were placed between the diode laser and the plate to prevent spurious electrical charge from reaching the diode laser. As an added precaution, a grounding strap was also mounted onto the plate itself. Due to the size and weight of the CCD camera, a mount was placed underneath the camera to remove the burden of weight from the echelle spectrograph. This avoids the possibility that the camera mount might pull away from the spectrograph over time.

As a safety consideration, the diode laser was encased within a steel enclosure. A small length of 50- μ m optical fiber is mounted within the enclosure and transports the laser light to a bulkhead on the side of the enclosure. Similarly, a small piece of fiber is mounted within the echelle spectrograph and transports the Raman signal from the exterior to the collimating lens. These optical fibers eliminate the need for either enclosure to be opened during field use.

The fiber-optic Raman probe can be directly connected to the fiber union bulkheads on the laser container and the echelle spectrograph. Alternatively, fiber-optic cable may be attached to the laser box and echelle spectrograph to allow the Raman probe to be taken into a remote area. The utilization of fiber-optic unions gives the system greater flexibility, allowing only the needed cable to be employed, minimizing throughput losses. The use of cable in this manner is also more cost effective, since a broken fiber does not require a complete realignment of the system. Testing at EIC Laboratories on the efficiency of these fiber-optic unions demonstrated that throughput losses were minimal ($< 1\%$).

The echelle spectrograph presents the Raman spectrum as a two-dimensional image on the CCD chip. However, the data presented to the end user should be presented as a single spectrum. Two considerations which deserved attention were the problems of properly calibrating each echelle order and determining the place and position at which echelle order $n-1$ should be spliced to echelle order n . The cutoff points for the free spectral range are defined by the optical equations. A method by which these cutoff positions can be directly related to precise positions on the CCD silicon wafer was needed.

A specialized computer software program was developed to accomplish the required tasks. The software consists of three important routines. The first of these, MANCAL.EXE, performs the initial calibration of the echelle spectrograph. The computer gives the frequency of a series of known lamp emission lines and their corresponding pixel position on the CCD chip are entered in MANCAL.EXE. This file of calibration points is then stored and used for calibration of collected data. The calibration of a collected spectrum is done using the program POSTPRO.EXE.

Raman spectra are recorded in terms of frequency differences from the frequency of the laser line. Since different laser sources can be employed, different echelle orders can be on the CCD chip. Therefore, it is necessary to know accurately the frequency of the laser line and the number of the initial echelle order before calibration. These parameters are maintained in the file

PARAM.DAT. If the wavelength of operation of the diode laser is changed, then the new laser wavelength would have to be placed into the PARAM.DAT file. The MANCAL.EXE program, however, would not have to be run again.

The efficiency of each echelle order maximizes at the center of each free spectral range and decreases as the edges of the free spectral range are approached. This leads to the appearance of a bowed background on each echelle order. This bowed background is removed by normalizing the data against a white light efficiency spectrum. This white light spectrum not only normalizes the grating efficiency function but the edge filter efficiency functions as well. The white light emission spectrum for the prototype unit is displayed in Figure 24.

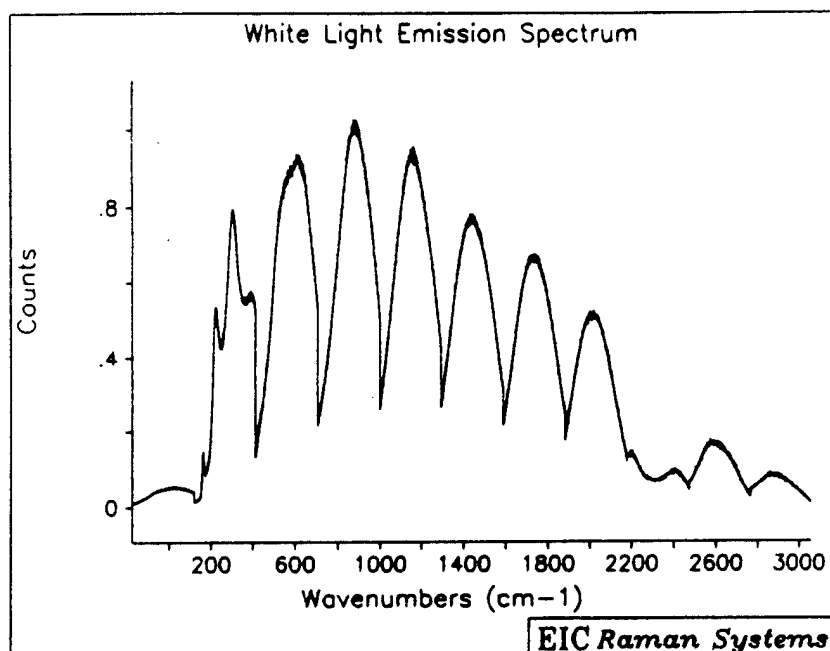


Figure 24. White Light Emission Spectrum from the Echelle Spectrograph and Fiber-Optic Raman Probe.

EIC Laboratories has developed a software routine which will automatically normalize the calibrated Raman spectrum against the white light efficiency spectrum. This program is a Lab Calc[®] macro (macro j) which allows multiple Lab Calc[®] functions to be called automatically. The macro program automatically imports the calibrated spliced ascii file (SPECTRUM.ASP) and converts it to the Lac Calc[®] specified format (SPECTRUM.SPC). Once in the appropriate format, the file is normalized against the stored white light spectrum and then displayed.

Once calibration and collection of the white-light instrument response function has been performed, emission spectra from standard lamp sources were collected. These emission spectra allow several characteristics to be evaluated simultaneously. First, the emission lines from these lamps were the ones utilized in the calibration routine and allow verification of a proper calibration. Second, intensity levels for the lamps can be compared to other instruments. Third, a plethora of lines are present in the emission lines and would quickly demonstrate a discrepancy if there was a gap in the spliced Raman spectrum. The emission spectra are displayed in Figures 25-29.

The spectra of the emission lines demonstrated that the system was properly calibrated. The throughput levels and resolution appeared to be as expected. In addition, there did not appear to be any emission lines missing indicating that the echelle spectrograph was collecting and displaying the entire Raman spectrum. The next step was to collect the Raman spectra of some Raman standards. Two of the Raman standards are presented in Figures 30 and 31.

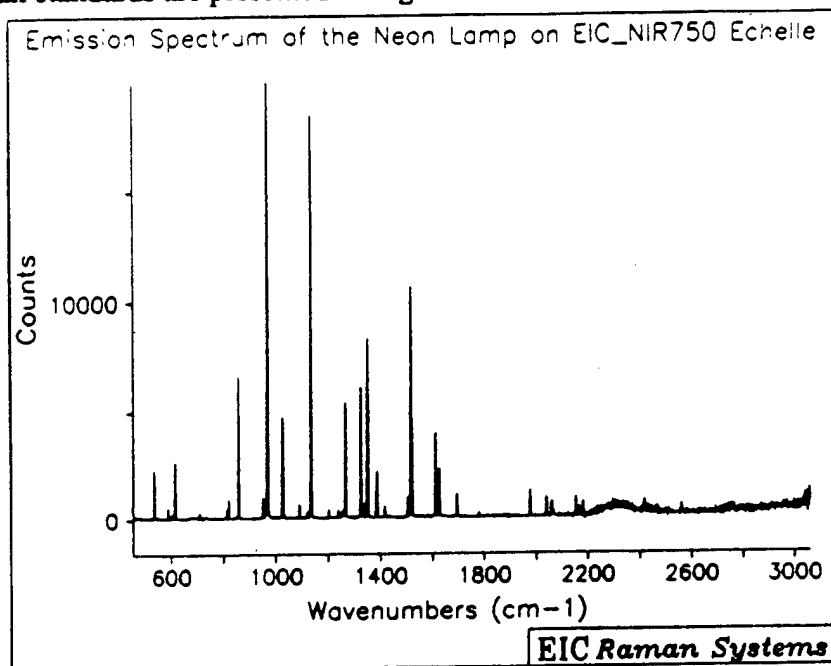


Figure 25. Emission Spectrum from a Neon Lamp Collected on the Prototype Echelle System.

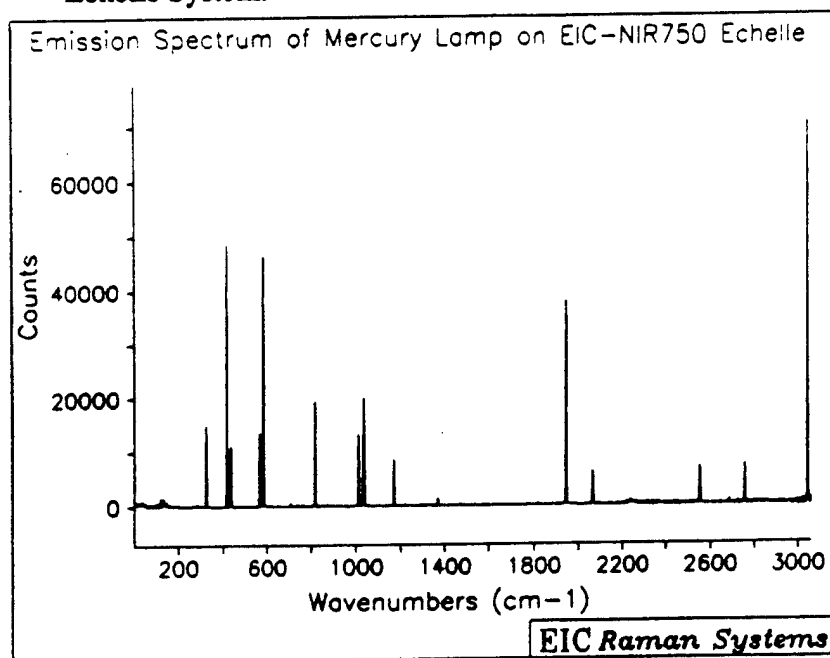


Figure 26. Emission Spectrum from a Mercury Lamp Collected on the Prototype Echelle System.

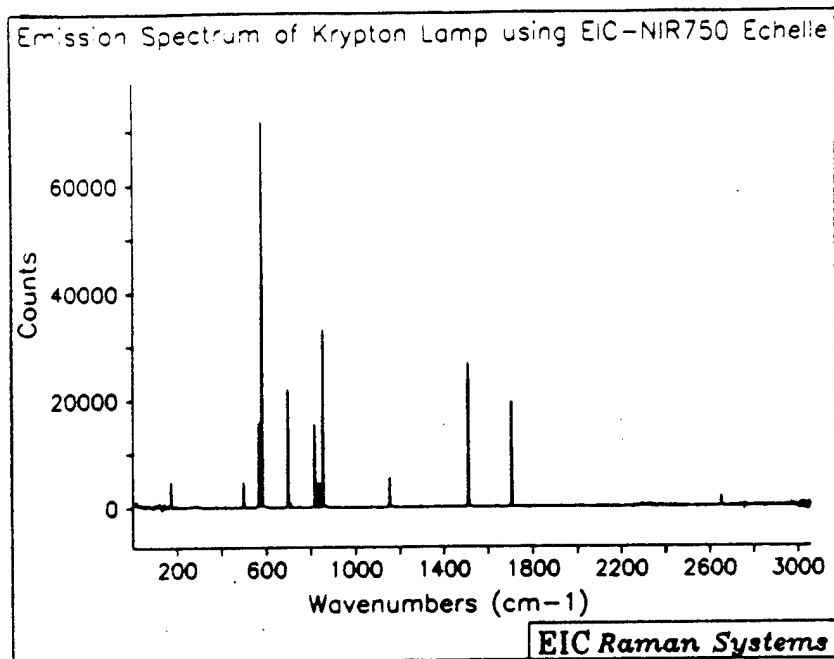


Figure 27. Emission Spectrum from a Krypton Lamp Collected on the Prototype Echelle System.

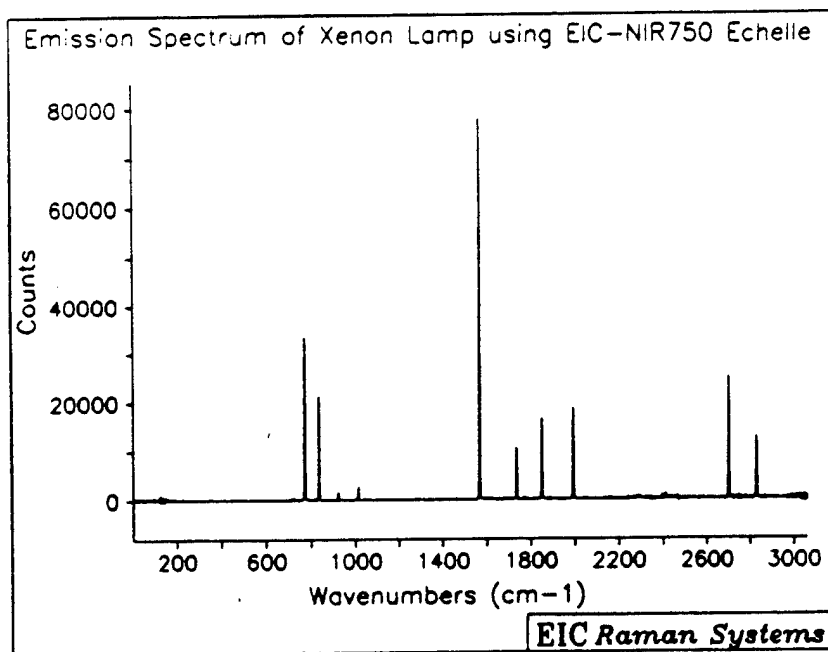


Figure 28. Emission Spectrum from a Xenon Lamp Collected on the Prototype Echelle System.

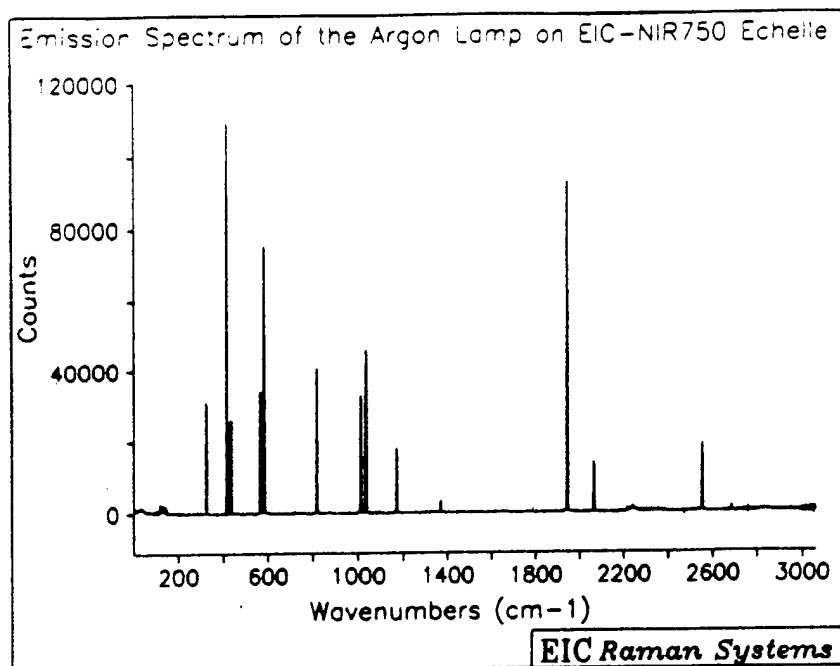


Figure 29. Emission Spectrum from a Argon Lamp Collected on the Prototype Echelle System.

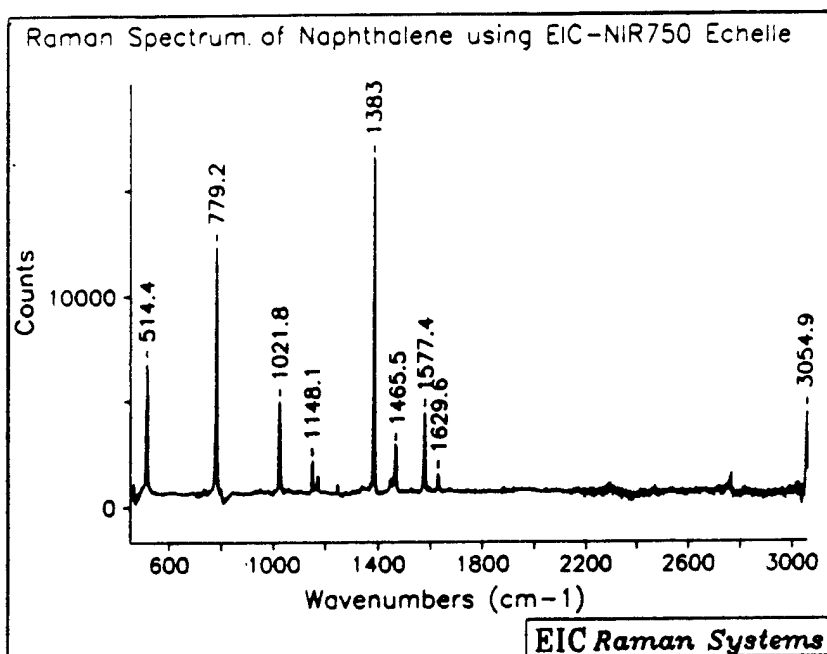


Figure 30. Raman Spectrum of Naphthalene Collected on the Prototype Echelle System.

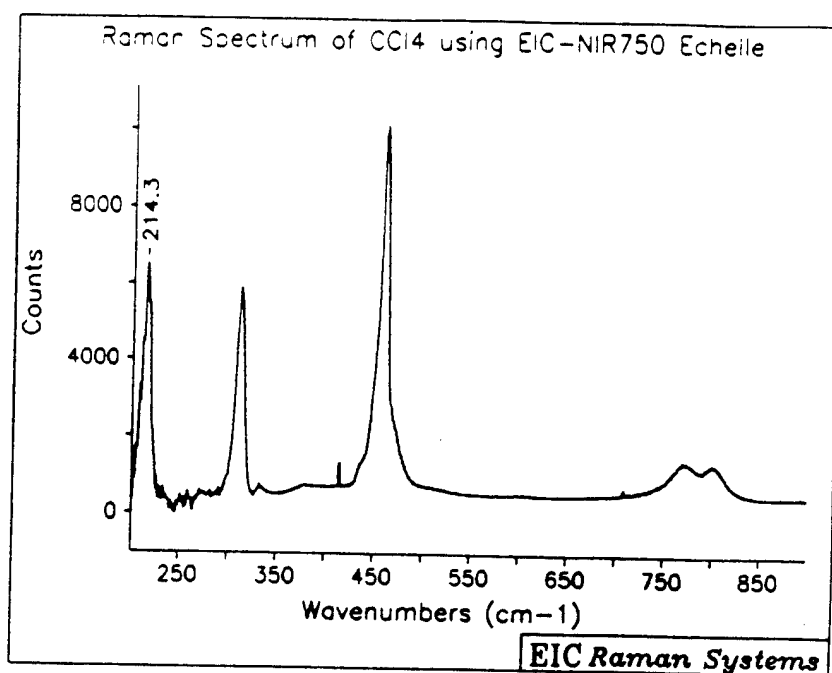


Figure 31. Raman Spectrum of Carbon Tetrachloride Collected on the Prototype Echelle System.

The Raman spectrum of naphthalene showed Raman spectra could be collected on the prototype echelle using the diode laser. The Raman spectrum of carbon tetrachloride demonstrated that Raman peaks down to 200-cm^{-1} could be collected. There was a larger background than desired in the $200\text{-}300\text{-cm}^{-1}$ region. The background can be traced to background emissions from the diode laser which have not been completely removed by the bandpass filter in the Raman probe. This can be improved by specifying a narrower bandpass filter for future Raman probes. For the current application, where the SERS bands of interest are in the $600\text{-}1400\text{-cm}^{-1}$, this minor revision is not necessary.

The SERS insert was next attached to the Raman probe and SERS spectra of the hazardous gases of interest were collected. These spectra are presented in Figures 32-34. The SERS spectrum of UDMH was collected at a higher concentration level than normal to allow the collection of a detailed spectrum. At lower concentrations, several of these Raman features are lost. The SERS spectra of NO_2 and SO_2 were collected at the standard 48-ppm. The signal-to-noise ratios on these spectra are excellent and indicate that high ppb detection is feasible with the current instrument and future improvements should allow detection of 100-ppb concentrations rapidly.

The results demonstrate that the prototype instrument operated as expected and it can collect Raman spectra. With the SERS insert and with properly conditioned preroughened and oxidized silver substrates, ppm detection of the hazardous gases of interest is feasible. This instrument is a prototype and certain revisions will be necessary. With further improvements, the instrument will achieve lower detection limits. In its current state, the prototype is of high enough quality to be utilized in preliminary field tests.

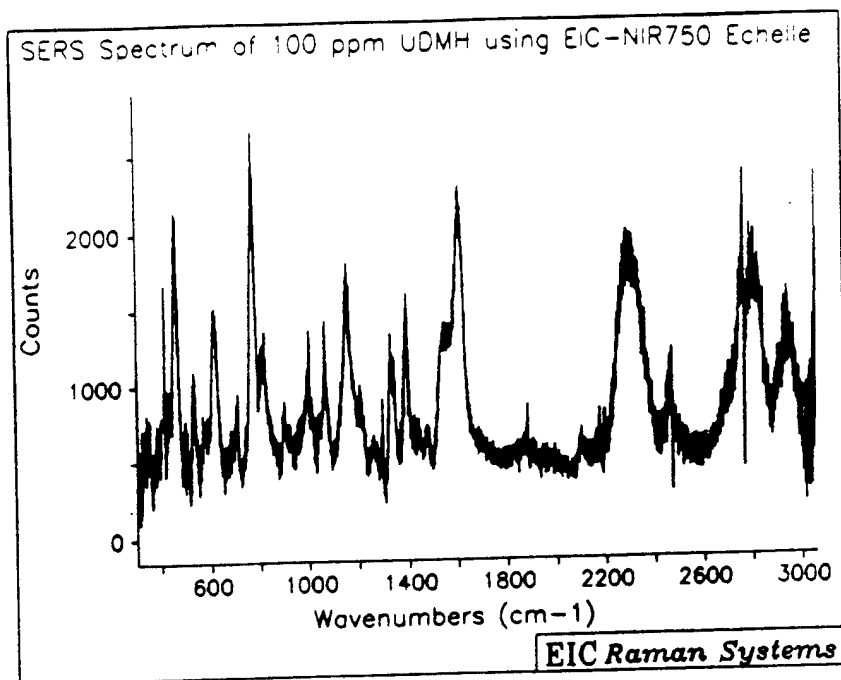


Figure 32. SERS Spectrum of 150-ppm UDMH Collected on the Prototype Echelle System with the SERS Insert.

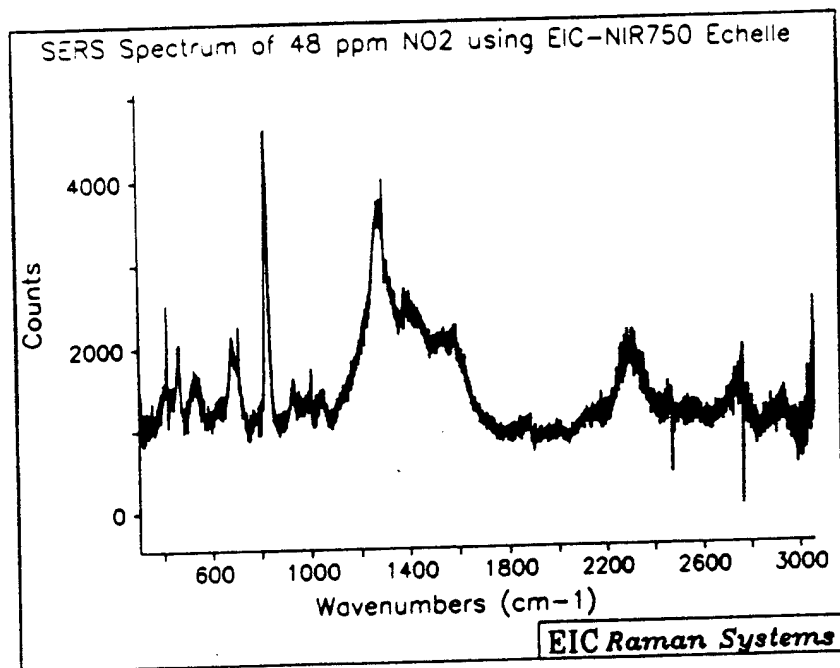


Figure 33. SERS Spectrum of 48-ppm NO₂ Collected on the Prototype Echelle System with the SERS Insert.

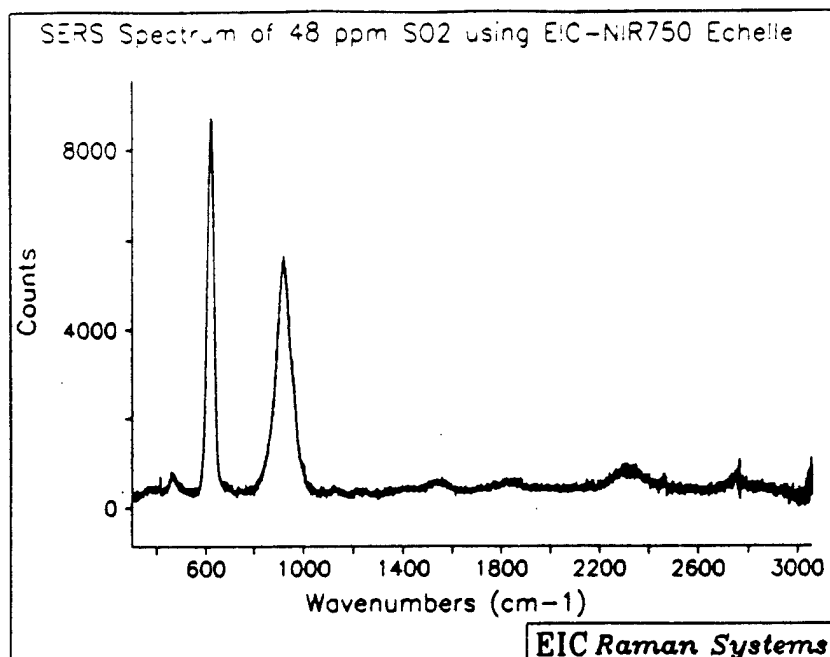


Figure 34. SERS Spectrum of 48-ppm SO₂ Collected on the Prototype Echelle System with the SERS Insert.

A complete analysis of instrument lifetime was not accomplished during the Phase II program. The echelle Raman system is designed for easy replacement of parts, so there should never arise the need to replace an entire system. Optical components are well protected within the spectrograph and should last for many years before coating degradations are observed, even in environments containing ppm levels of mildly corrosive gases. Electronic failures are expected to occur more frequently and could manifest themselves in CCD controller circuitry, diode laser circuitry, or in the computer. All three may be easily and inexpensively repaired. The diode laser is expected to have a 2000 h lifetime and will have to be replaced. This is anticipated to be the most common maintenance to be performed on the NIR echelle Raman system. The only other routine maintenance to anticipate is vacuum loss by the CCD dewar system. The vacuum loss occurred less than once a year and utilization of a non-oil-based vacuum pump would restore the vacuum.

Long term instrument cost is ill defined. The cost of CCD detectors, one of the prime instrument cost factors, has dramatically declined over the past two years. The price drop is >50% of the CCD utilized on this prototype. The diode laser market is also in a state of flux and estimation of future cost is difficult. There are also instrumental improvements to be performed which will change the overall price of the commercial unit. In particular, replacement of the commercial lenses with custom fabricated lenses to optimize system throughput will change echelle spectrograph cost and will be highly dependent upon the volume of sales.

SECTION V

CONCLUSIONS

The results of the Phase II program demonstrate that an SERS-Based echelle spectroscopic system for ppb detection of hazardous gases is feasible and should proceed to preliminary field tests. The following conclusions can be made from the Phase II results:

- An SERS substrate with a defined internal standard is desirable. However, a more detailed investigation is needed to produce a standard which does not corrupt the enhancement capabilities of the SERS substrate;
- Electrochemical roughening and oxidation had similar reproducibility to substrates prepared by vacuum deposition. This is most likely caused by inadequate control over operating parameters and contaminants in a shared sputtering system;
- SERS signal strength was strongest in the NIR and silver was the most sensitive and reproducible SERS metal;
- Diode lasers in the 670 and 780-nm region were unstable due to optical feedback arising from the fiber coupling. Utilization of an optical isolator appeared to improve diode stability, although the future of diode lasers as the portable laser source is uncertain;
- Backscattered SERS signals appeared to be as strong as, if not stronger, than corresponding SERS signals collected at a 90° angle;
- The echelle spectrograph was capable of collection of the desired spectral range simultaneously;
- Commercial NIR camera lenses did not appear to have a wide enough clear aperture to allow the entire CCD chip width to be utilized unimpeded. The echelle had to be operated in a demagnification configuration to collect the full echelle order widths. The demagnification allowed complete collection of the Raman spectrum while simultaneously improving throughput.
- Collection of SERS spectra on the prototype instrument was demonstrated to be feasible.

SECTION VI

RECOMMENDATIONS

There are several investigations to be performed which can improve the quality and usefulness of the prototype SERS monitor of gaseous contaminants. One immediate need is to increase the gaseous SERS spectrum database. A choice to study a few compounds in detail was made for maximum understanding of the basic detection scheme. Although there are other basic experiments that could be performed on these compounds, we recommend diversity at this juncture. SERS spectra of other gaseous contaminants collected during the Phase I program, such as H_2S or NH_3 , should be extended to the echelle system. Compounds not studied during this program should also be investigated, such as the breakdown products of hydrazine, MMH, and UDMH; hydrogen peroxide, diazene, N_2O , and HONO (Tuazon, 1988). The prototype echelle system could also be utilized for detection of gaseous solvents, such as benzene, in enclosed areas and serve as an indoor air quality monitoring system. Collection of SERS spectra from new compounds will require investigation into the optimum methods for substrate preparation for each compound.

Expansion of the prototype echelle system to multiple SERS probe deployment is recommended. Since different oxide layers are required for maximum detection of the studied hazardous gases, it is desirable to have SERS substrates for each gas to be studied present at the deployment site. One option is to have several SERS inserts placed at strategic locations and then to manually transfer a single Raman probe between the inserts to obtain the desired information. Another option would be to have several Raman probes with SERS inserts in the field and use an automated multiplexer system for continuous sequential scanning of the deployed probes. This could be accomplished through the use of a motorized stage at the laser source which would move the different excitation fibers into the diode laser focal plane. A similar approach could be utilized for the collection fibers prior to the echelle entrance or a fiber-optic multiplexer could be used.

Research should be pursued on improved manufacturing methods for the SERS substrates. Either vacuum deposition or electrochemical roughening of electrodes followed by an appropriate oxidation stage provided sensitive SERS substrates. It would be desirable to improve the quantitative nature of the SERS technique. These substrates currently give signal levels that can be reproduced to within a factor of 2-3. The current limiting factor is control over the surface morphology. Future research should be directed towards improved quality control over the substrate surfaces. This will require basic research into understanding the mechanism of surface roughening.

Further revisions of the prototype echelle lens system should be pursued. Customized NIR imaging lenses should allow the desired 1-cm^{-1} resolution at high throughput. These lenses should also improve the resolution of the current spectrograph by a factor of 2-3, have 2 times the throughput in the orders near the laser line (echelle order 44) with increasing throughput improvements as the wavelength approaches $1\text{-}\mu\text{m}$ (echelle order 34).

Future investigations of the portable laser market and the CCD market are recommended. Investigations of several diode lasers from multiple manufacturers has yet to find a diode laser that is completely satisfactory for a field portable unit. Although problems in diode laser stability may be alleviated in the near future, other possible NIR laser sources for portable systems should be investigated.

The CCD employed on the prototype echelle system drops rapidly in sensitivity across the NIR spectral range probed. Improved sensitivity can be obtained by "back thinning" the silicon CCD wafer. Sensitivity doubling has been demonstrated with such enhanced CCD detectors (Sweedler, 1988). However, mass production of the special silicon wafer has not been successfully accomplished. When these wafers are available and are proven capable of field deployment, implementation of this camera into the prototype echelle is recommended.

Finally, we recommend an investigation of the delivered echelle Raman prototype for other applications. The echelle Raman system is a complete instrument which can be utilized in a variety of applications. When fitted with copper substrates, the EIC SERS probe can detect organic chlorides in groundwater, as well as bacterial species (Carrabba, 1992). Other properly designed SERS substrates should be capable of detecting trace quantities of military ordnance or warfare agents.

The Raman probe can be decoupled from the SERS housing and can be utilized to detect Raman scattering. Although not capable of trace detection, Raman spectroscopy can be utilized in a wide variety of applications requiring remote analysis. Analysis of corrosion products on coated and uncoated surfaces can be performed. Raman spectroscopy can be used for waste analysis (Carrabba, 1992). Raman spectroscopy can be used for quality control applications as well. For example, the Raman probe could be utilized to detect variations in jet fuel composition. Raman spectroscopy is an excellent technique since every compound provides a unique fingerprint and should be tested for multiple Air Force applications.

BIBLIOGRAPHY

- Angel, S., and Myrick, M., Appl. Spectrosc., Vol. 44, p. 565, 1990.
- Bond, G., Catalysis by Metals, Academic Press, New York, 1962.
- Carrabba, M. and Rauh, R., "Remote Fiber-Optic Sensor for Gaseous and Liquid Environments Based on Surface-enhanced Raman Spectroscopy-(SERS)," N00014-87-C-0859(F), Office of Navy Research, March, 1988.
- Carrabba, M., "Surface-enhanced Raman Spectroscopy (SERS) An Existing or Emerging Chemical Sensing Technology?," paper presented at the Department of Energy *In Situ* Characterization and Monitoring Technologies Workshop, Idaho Falls, ID, June, 1988.
- Carrabba, M., Edmonds, R., Marren, P., and Rauh, R., "The Suitability of Surface-enhanced Raman Spectroscopy (SERS) to Fiber-Optic Chemical Sensing of Aromatic Hydrocarbon Contamination in Groundwater," Field Screening Methods for Hazardous Waste Sites Investigations, U.S. Environmental Protection Agency, p. 33, 1988.
- Carrabba, M., Edmonds, R., Rupich, M., Marren, P., and Rauh, R., "Fiber-Optic SERS for Chemical Sensing of Gaseous and Liquid Environments," paper presented at 15th FACSS Meeting, Boston, MA, October 1988.
- Carrabba, M., Spencer, K., Rich, C., and Rauh, R., Appl. Spectrosc., Vol. 44, p. 1558, 1990.
- Carrabba, M., "Fiber-Optic Raman Spectroscopy for Environmental Monitoring," paper presented at SAME-Technology Transfer Conference on Environmental Cleanup, Denver, CO, November, 1991.
- Carrabba, M. and Spencer, K., "A Nonintrusive Monitor for Biocorrosion/Biofouling of Coated Materials," N60921-91-C-0156, Naval Surface Warfare Center, May, 1992.
- Carrabba, M., Spencer, K., Edmonds, R., Rauh, R. and Haas, J., SPIE OE/LASE'92-Laser Spectroscopy, Vol. 1637, p. 82, 1992.
- Carrabba, M., and Rauh, R., "Apparatus for Measuring Raman Spectra Over Optical Fibers", U.S. Patent, 5,112,127 (1992).
- Carrabba, M., Spencer, K., Edmonds, R., and Haas, J., "Applications of Fiber-Optic Raman Spectroscopy to Environmental Monitoring," paper presented at 19th FACSS Meeting, Philadelphia, PA, September 1992.
- Chang, R. and Furtak, T. eds., Surface-enhanced Raman Scattering, Plenum Press, New York, 1982.
- Dorain, P., von Raben, K., Chang, R., and Laube, B., Chem. Phys. Lett., Vol. 84, p. 405, 1981.

Sweendler, J., Bilhorn, R., Epperson, P., Sims, G., and Denton, M., Anal. Chem., Vol. 60, p. 282A, 1988.

Fleischmann, M., Hendra, P., and McQuillan, A., "Raman Spectra of Pyridine Adsorbed at a Silver Electrode," Chem. Phys. Lett., Vol. 26, p. 163, 1974.

Garrell, R., "Surface-enhanced Raman Spectroscopy," Anal. Chem., Vol. 61, p. 401A, 1989.

Gileadi, E., Electrosorption, Plenum Press, New York, 1977.

Hayashi, S., Surf. Sci., Vol. 158, p. 229, 1985.

Jennings, C., Aroca, R., Hor, A., and Loutfy, R., Anal. Chem., Vol. 56, p. 2033, 1984.

Pockrand, I., Surface Enhanced Raman Vibrational Studies at Solid/Gas Interfaces, Springer-Verlag, Berlin, 1984.

Snow, A. and Rose, S., "Review of Specific Chemical Interactions for Hydrazine Analysis and Proposed Adaptation for Microsensor Chemical Detection," Memorandum Report 5461, Naval Research Laboratory, November, 1984.

Tuazon, E., and Carter, W., paper presented at the Third Conference on the Environmental Chemistry of Hydrazine Fuels, Panama City Beach, FL, September, 1987.